Ebullition was a major pathway of methane emissions from the aquaculture ponds in southeast China

Yang, P., Zhang, Y., Yang, H. ORCID: https://orcid.org/0000-0001-9940-8273, Guo, Q., Lai, D. Y. F., Zhao, G., Li, L. and Tong, C. (2020) Ebullition was a major pathway of methane emissions from the aquaculture ponds in southeast China. Water Research, 184. 116176. ISSN 0043-1354 doi: 10.1016/j.watres.2020.116176 Available at https://centaur.reading.ac.uk/95933/

It is advisable to refer to the publisher's version if you intend to cite from the work. See [Guidance on citing](#).

www.reading.ac.uk/centaur

Ebullition was a major pathway of methane emissions from the aquaculture ponds in southeast China

Ping Yang[ab], Yifei Zhang[ab], Hong Yang[cde], Qianqian Guo[ab], Derrick Y.F. Lai[f], Guanghui Zhao[a], Ling Li[a], Chuan Tong[ab]

[a] Key Laboratory of Humid Subtropical Eco-geographical Process of Ministry of Education, Fujian Normal University, Fuzhou, 350007, China
[b] School of Geographical Sciences, Fujian Normal University, Fuzhou, 350007, China
[c] College of Environmental Science and Engineering, Fujian Normal University, Fuzhou, 350007, China
[d] Collaborative Innovation Center of Atmospheric Environment and Equipment Technology, Jiangsu Key Laboratory of Atmospheric Environment Monitoring and Pollution Control (AEMPC), School of Environmental Science and Engineering, Nanjing University of Information Science & Technology, 219 Ningliu Road, Nanjing, 210044, China
[e] Department of Geography and Environmental Science, University of Reading, Whiteknights, Reading, RG6 6AB, UK
[f] Department of Geography and Resource Management, The Chinese University of Hong Kong, Shatin, New Territories, Hong Kong SAR, China

Abstract

Aquaculture ponds are hotspots of carbon cycling and important anthropogenic sources of the potent greenhouse gas methane (CH_4). Despite the importance of CH_4 ebullition in aquatic ecosystems, its magnitude and spatiotemporal variations in aquaculture ponds remain poorly understood. In this study, we determined the rates and spatiotemporal variations of ebullitive CH_4 emissions from three mariculture ponds during the aquaculture period of two years at a subtropical estuary in southeast China. Our results showed that the mean ebullitive CH_4 flux from the studied ponds was 14.9 mg CH_4 m^{-2} h^{-1} during the aquaculture period and accounted for over 90% of the total CH_4 emission, indicating the importance of ebullition as a major CH_4 transport mechanism. Ebullitive CH_4 emission demonstrated a clear seasonal pattern, with a peak value during the middle stage of aquaculture. Sediment temperature was found to be an important factor influencing the seasonal variations in CH_4 ebullition. Ebullitive CH_4 fluxes also exhibited considerable spatial variations within the ponds, with 49.7–71.8% of the whole pond CH_4 ebullition being detected in the feeding zone where the large loading of sediment organic matter fueled CH_4 production. Aquaculture ponds have much higher ebullitive CH_4 effluxes than other aquatic ecosystems, which indicated the urgency to mitigate CH_4 emission from aquaculture activities. Our findings highlighted that the importance of considering the large spatiotemporal variations in ebullitive CH_4 flux in improving the accuracy of large-scale estimation of CH_4 fluxes in aquatic ecosystems. Future studies should be conducted to characterize CH_4 ebullitive fluxes over a greater number and diversity of aquaculture ponds and examine the mechanisms controlling CH_4 ebullition in aquatic ecosystems.

1. Introduction

Rising concentrations of atmospheric greenhouse gases since the beginning of the industrial era are of international concern owing to their huge implications to climate change

(IPCC, 2019; Tangen et al., 2016). Methane (CH_4) is a potent greenhouse gas that has a sustained-flux global warming potential of 45 times higher than that of CO_2 on a per mass unit basis over a 100–year time horizon (Neubauer and Megonigal, 2015), and contributes to approximately 20% of the global radiative forcing (IPCC, 2013). Global average atmospheric CH_4 concentration has increased from 722 ppb in 1750 to 1875 ppb in 2019 (National Oceanic and Atmospheric, 2020), exceeding the pre-industrial levels by about 150%. Thus, determining the sources, magnitude, and mechanisms of CH_4 emissions around the world is crucial for mitigating global climate change and the associated adverse effects on the environment and human society.

Aquatic systems are potentially significant contributors to global CH_4 emissions. Previous studies have reported that inland waters including rivers (Borges et al., 2015; Yuan et al., 2019), lakes (Bastiviken et al. 2011; Tangen et al., 2016; Yang et al., 2011), reservoirs (Musenze et al., 2014; Yang et al., 2012) are strong sources of atmospheric CH_4. Small ponds, especially those perturbed by humans, form an indispensable part of the global inland water systems, and play an important role in the biogeochemical cycling of carbon and the release of CH_4 (Holgerson, 2015; Holgerson and Raymond, 2016; Rubbo et al., 2006; Yuan et al., 2019). Over the past two decades, large efforts have been made to evaluate the concentrations, fluxes, and drivers of CH_4 in small ponds from different countries, including Sweden (Bastviken et al., 2004; Natchimuthu et al., 2014; Peacock et al., 2019), Germany (Ortega et al., 2019), Canada (Hamilton et al., 1994; Laurion et al., 2010; Pelletier et al., 2014), India (Panneer Selvam et al., 2014), the USA (Holgerson, 2015; Gorsky et al., 2019), Netherlands (van Bergen et al., 2019) and Australia (Grinham et al., 2018a). Aquaculture ponds form an important component of the global man-made aquatic ecosystems. The freshwater and brackish aquaculture ponds, with a global total surface area of around 1.1×10^5 km^2 (Verdegem and Bosma, 2009), are potential hotspots of CH_4 emission because of their large loadings of organic matter from residual feeds and feces of cultured animals (IPCC, 2019; Yang et al., 2018, 2019; Yuan et al., 2019). Although numerous studies have quantified CH_4 fluxes from the aquaculture ponds (Chen et al., 2016; Ma et al., 2018; Soares and Henry-Silva, 2019; Wu et al., 2018; Yang et al., 2018, 2019; Yuan et al., 2019), the biogeochemical processes involved (e.g., CH_4 production, oxidation, and transport) in the aquaculture systems have thus far received little attention (Avnimelech and Ritvo, 2003).

Biogenic CH_4 is produced during the terminal step of organic matter degradation in anaerobic sediments (Lofton et al., 2015) and in oxic waters with rich planktonic microbes (Bogard et al., 2014; Khatun et al., 2019; Tang et al., 2016). CH_4 can be exported from the sediment to the atmosphere through gas ebullition, molecular diffusion, or plant-mediated transport (Bastviken et al., 2004, 2008; Wu et al., 2019; Yang et al., 2015). The majority of existing studies determined the diffusive CH_4 fluxes from aquatic ecosystems based on the wind-based estimations of gas transfer velocity (piston velocity, k) along with measurements of surface water CH_4 concentrations (Borges et al., 2018; Cole and Caraco, 1998; Cotovicz et al., 2016). On the other hand, CH_4 ebullition in freshwater systems (e.g., lakes, reservoirs, ponds) has traditionally been measured by directly capturing the released bubbles with inverted funnels (Davidson et al., 2018; Wik et al., 2013; Zhou et al., 2019) or indirectly with the use of floating chambers (*FCs*) (Bastviken et al., 2004; Chuang et al., 2017; Natchimuthu et al., 2014; Wu et al., 2019). To estimate the ebullition, the total CH_4 flux from the non-vegetated water bodies measured by the *FCs* are compared against the diffusive CH_4 flux determined by the gas transfer coefficient method (Bastviken et al., 2004; Chuang et al., 2017; Natchimuthu et al., 2014; Wu et al., 2019).

Although the upscaling of chamber-based CH_4 fluxes is subjected to potential bias when ebullition rates are spatially heterogeneous, *FCs* have been widely used in flux measurement owing to their low cost and relative ease of operation (Bastviken et al., 2015; Lorke et al., 2015; Podgrajsek et al., 2014). Recently, some state-of-the-art techniques, such as hyperspectral image analysis (Gålfalk et al., 2016), optical detectors (Grinham et al., 2011), hydroacoustic (sonar) technology (DelSontro et al., 2011) and automated bubble traps (Maher et al., 2019), have also been employed to measure CH_4 ebullition.

Ebullition is often considered as a dominant CH_4 emission pathway in the shallow area of reservoirs (Deshmukh et al., 2016), rivers (Wu et al., 2019), and lakes (Bastviken et al., 2004; Natchimuthu et al., 2016; Xiao et al., 2017). However, the magnitude of CH_4 ebullition can vary from time to time both within and across ecosystems depending on the CH_4 production rate (Zhou et al., 2019), trophic state (Bastviken et al., 2008; Walter et al., 2008; Zhou et al., 2019), water depth, and other environmental factors (e.g., water temperature and atmospheric pressure) (Maeck et al., 2014; Zhu et al., 2016). Organic matter in sediment is a major source of substrate for CH_4 production in aquatic ecosystems (Bastviken et al., 2008; Walter et al., 2008; Zhu et al., 2016). CH_4 ebullition generally increases with organic matter content (DelSontro et al., 2011; Zhou et al., 2019; Zhu et al., 2016), but this process is highly stochastic (Bastviken et al., 2004) with large spatiotemporal variations (e.g., DelSontro et al., 2011; Natchimuthu et al., 2016; Wilkinson et al., 2015). Recent studies have suggested that ebullition could dominate CH_4 emissions from shallow ponds (e.g., Natchimuthu et al., 2014; Yang et al., 2019a). Without *in situ* sampling and observation, the magnitude and spatiotemporal variations of ebullitive CH_4 fluxes in aquaculture ponds remain largely unknown, which limit our ability in accurately determining CH_4 fluxes from shallow ponds and their contributions to the global CH_4 budget.

China has the largest area of aquaculture ponds in the world (approximately 25,700 km^2; 23% of the global total), with many of them being widely located in the subtropical estuaries along the coastal regions (Ren et al., 2019; Yang et al., 2018). Shrimp mariculture is one of the dominant types of land-based aquaculture in the coastal areas of China (Yang et al., 2017a). These shrimp ponds are generally maintained through daily supply of feeds (Yang et al., 2017a), with a rather low feed utilization efficiency in the range of ~4.0% - 27.4% (Chen et al., 2015; Molnar et al., 2013). Consequently, the majority of the uneaten feeds, along with animal excreta and dead phytoplankton, deposit on the sediment surface. The microbial decomposition of these organic-rich materials can stimulate CH_4 production and thereby contribute to a large amount of ebullitive CH_4 flux. However, the contribution of ebullitive CH_4 fluxes in aquaculture ponds is largely understudied, considering the enormous number and size of these ponds globally. Furthermore, mariculture ponds are largely affected by topography, environmental factors (e.g., sediment organic matter and temperature), and management practices (Yang et al., 2018; 2019). This could lead to considerable spatiotemporal variations in ebullitive CH_4 fluxes, which should be further characterized and tested by field observation.

To the best of our knowledge, this study made the first attempt to estimate ebullitive CH_4 fluxes from the intensive mariculture ponds. The intensity of mariculture pond culture has increased progressively over the last few decades (Wang et al., 2018). Intensive shrimp pond is the most dominant type of land-based aquaculture ponds in the coastal region in China with an area of 2.4×10^3 km^2 (Bureau of Fisheries of the Ministry of Agriculture, 2019), accounting for approximately 12% of the total global area of shrimp aquaculture ponds. This research aimed to: (1) determine the magnitude, spatiotemporal variations, and main controls

of ebullitive CH_4 fluxes within the ponds; and (2) examine the relative contribution of ebullition to total CH_4 fluxes from the mariculture ponds. We hypothesized that: (1) ebullitive CH_4 fluxes would exhibit remarkable temporal variations in response to differences in environmental variables (e.g., temperature and substrate availability); (2) ebullitive CH_4 fluxes would vary significantly among different zones (nearshore area, feeding area, and aeration area) within the ponds owing to differences in oxygen and substrate supply; and (3) ebullition would contribute markedly to the total CH_4 emissions from the mariculture ponds owing to the large organic matter load and shallow water depth.

2. Materials and methods

2.1. Study area and shrimp pond system

The study was conducted in the intensive aquaculture ponds with monoculture of white shrimps (*Litopenaeus vannamei*) located at the Shanyutan Wetland in the Min River Estuary (MRE) southeast China (26°00′36″–26°03′42″N, 119°34′12″–119°40′40″E, Fig. 1). White shrimp is the most important type of maricultured crustacean species in China with an annual yield of approximately 875,000 tons, which is over 6 times higher than the yield of mud crab (Wang et al., 2018). Moreover, intensive shrimp is particularly dominant in the southern part of China (Yuan et al., 2006). Hence, our study ponds represented a very common management regime of mariculture ponds in the region. The study area is influenced by a subtropical monsoonal climate with annual mean temperature of 19.60 °C and annual precipitation of 1,350 mm (Tong et al., 2010). The total area of shrimp ponds at the Shanyutan wetland is about 234 ha (Yang et al., 2017a). These shrimp ponds were created in 2011 by complete removal of original marsh vegetations (Yang et al., 2017b). Field measurement was conducted in three selected ponds, which were representative of the physical setting and management practices of mariculture ponds in the surrounding region. These three ponds had a small size of 19,000 m^2, which was close to the range of 20,000–30,000 m^2 found in Thailand and Taiwan (Kongkeo, 1997) and 33,300–66,700 m^2 reported in Chinese shrimp ponds (Xie & Yu, 2007). Moreover, our ponds had shallow water depths ranging between 1.1 and 1.8 m over the culture period (Yang et al., 2019a), which were close to the mean of 1.7 m reported in tropical China (Herbeck et al., 2013) and 1.0 m in shrimp ponds across China (Cao et al., 2007).
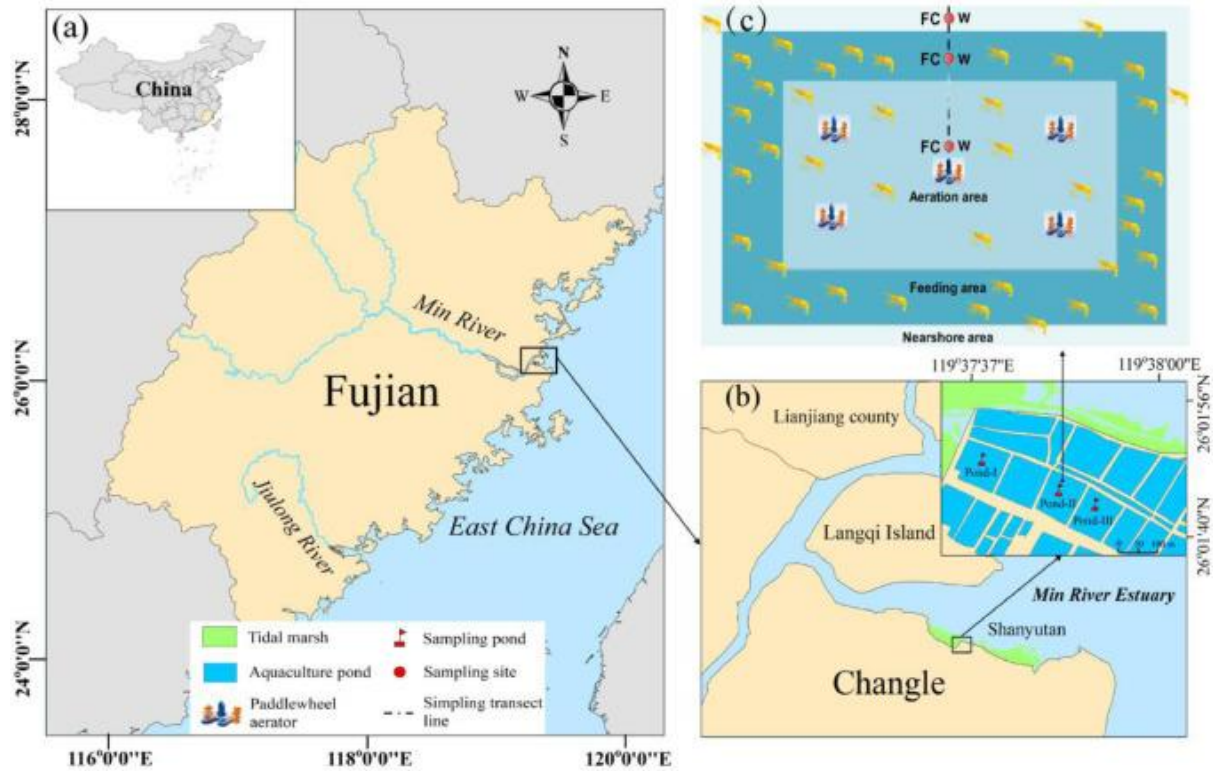
Fig. 1. (a) Location of the study area; (b) sampling sites and ponds in Shanyutan wetland of Min River estuary, southeast China; and (c) schematic diagram of aquaculture shrimp pond and the location of sampling sites (red dots). W = water samples; FC = flux measurement using floating chambers.

Shrimp aquaculture usually starts in June and ends in November, with only one single crop being produced each year (Yang et al., 2017a). Before the start of the production cycle, these ponds were filled with seawater from the Min River estuary using a submerged pump (Yang et al., 2018, 2019). There was no water exchange during the culture period, except occasional input by rainfall events. The stocking density of shrimps in our ponds was around 35–45 individuals m^{-2} (Yang et al., 2017a), which was comparable to 54 and 38–73 individuals m^{-2} in other intensive shrimp ponds in China (Xie & Yu, 2007), and the Philippines and Taiwan (Kongkeo, 1997), respectively. The shrimps were regularly fed with artificial feeds (Hangsheng and Tianma Chia Tai Feed Co., Ltd., Fuzhou, China) twice per day (07:00 AM and 16:00 PM, local standard time) manually from a boat. These pellet feeds have been commonly used in mariculture ponds across China (Wang et al., 2018). The feed conversion ratio in our ponds ranged between 1.11 and 1.72, which was lower than 2.1 reported in other intensive shrimp ponds in China (Xie and Yu, 2007) but similar to the range of 1.38–1.67 in other Asian countries including Indonesia, Taiwan and Thailand (Kongkeo, 1997). Generally, three to five automatic paddlewheel aerators were operated four times per day (00:00–03:00, 07:00–09:00, 12:00–14:00, and 18:00–20:00) to increase the oxygen content in water. Paddlewheel aerators are equipped in most of the intensive shrimp ponds in China and operated either continuously or a few hours in the day depending on weather (Herbeck et al., 2013). According to the spatial variations in microtopographic features, water depth, and management practices, the shrimp ponds were divided into three distinct zones, namely Zone N (near-shore area with sparse submerged vegetation), Zone F

(deep-water area for feeding activities) and Zone A (shallow-water area for aeration) (Fig. S1 and Table S1, Yang et al., 2019a; Zhang et al., 2019).

2.2. Experimental design

To determine the spatiotemporal variations in CH_4 emissions within the ponds during the culture period, we collected water, sediment, and gas samples from three replicate shrimp ponds at the Shanyutan Wetland (Fig. 1). A wooden bridge was built in each pond to facilitate the access to the sampling sites and minimize the potential disturbance to the pond ecosystem. Field sampling campaigns were carried out at all three zones (N, F, and A) in the ponds (Fig. 1) between June and November in 2017, and May and October in 2018 following the timing of aquaculture management practices. Gas fluxes were measured and water samples were taken 2–3 times each month. Sediment samples were collected during the initial (June or May), middle (August), and final (October) stages of shrimp production. On each sampling day, all samples were taken between 9:00 am and 11:00 am to minimize the potential discrepancies owing to diurnal variations (Chen et al., 2016; Wu et al., 2019;Zou et al., 2015).

2.3. Dissolved CH_4 concentration and diffusive CH_4 flux

Bubble-free water samples were collected at the depth of 20 cm using a gas-tight water sampler for dissolved CH_4 concentration analysis. Subsequently, 55-mL gas-tight serum glass bottles were flushed with the collected water samples thoroughly for three times before being completely filled with the water samples. Prior to sealing the bottles, approximately 0.2 mL of saturated $HgCl_2$ solution was injected into each sample to inhibit bacterial activity (Borges et al., 2018). The glass bottles were then immediately sealed without headspace using a halobutyl rubber septum to exclude any air bubbles (Borges et al., 2018; Xiao et al., 2017). The water samples were then stored in an ice-packed cooler, transported to the laboratory within 4–6 h, and analyzed within two days.

The concentrations of dissolved CH_4 in the water samples were determined using the headspace equilibrium technique and a gas chromatograph (GC-2010, Shimadzu, Kyoto, Japan) equipped with a flame ionization detector. Five CH_4 standards, namely 2, 8, 500, 1000, and 10,000 ppm, were used in the calibration. The CH_4 detection limit was 0.3 ppm, and the relative standard deviations of CH_4 analyses were ≤ 2.0% in 24 h. Details about the gas sampling procedures and configurations of the gas chromatograph can be found in our previous paper (Yang et al., 2019a). The *in situ* dissolved CH_4 concentration in surface water (C_{waer}) was calculated based on CH_4 concentration in the headspace of the glass bottles after equilibration (Eq. (1); Hu et al., 2018):

$$(1) C_{Water} = [(C_H − C_A) \times V_H + \alpha \times C_H \times V_W]/V_W$$

where C_H is CH_4 concentration (μmol L^{-1}) in the headspace of the glass bottles at equilibrium; C_A is the atmospheric CH_4 concentration (μmol L^{-1}) at the prevailing *in situ* conditions; V_H is the volume of headspace gas in the glass bottles (L); α is the Bunsen coefficient (Wanninkhof, 1992); and V_W is the volume of water in the glass bottles (L).

The diffusive CH_4 fluxes (F_D, μmol m^{-2} h^{-1}) across the water-atmosphere interface were calculated based on the gas transfer coefficient method (Eq. (2); Musenze et al., 2014; Xiao et al., 2017):

$$(2) F_D = k_x \times (C_{Water} − C_{Eq})$$

where C_{Water} (μmol L^{-1}) is the dissolved CH_4 concentration measured at the water surface; C_{Eq} (μmol L^{-1}) is the CH_4 concentration in

equilibrium with the atmospheric concentration at the prevailing *in situ* conditions; and k_x is the gas transfer velocity (cm h^{-1}). In the present study, we report the unit of CH$_4$ diffusive flux as mg m^{-2} h^{-1} (= $F_D \times M \times 10^6$), where M is molar mass of CH$_4$ (16 mg mol^{-1}).

Considering the influence of varying wind speeds on the estimated k_x value, we adopted the model of Cole and Caraco (1998), which was developed under wind conditions most similar to our studied aquaculture ponds, to calculate k_x values : (3)$k=(Sc/600)-0.5\times(2.07+0.215\times U10 1.7)$where Sc is the Schmidt number for CH$_4$ corrected by *in situ* water temperature (Jahne et al., 1987; MacIntyre et al., 1995; Xiao et al., 2017); and U_{10} is the frictionless wind speed at 10 m height (m s^{-1}) according to Eq. (4) (Musenze et al., 2014; Sibgh et al., 2007):(4)$U10=Uz[1+(Cd10)1/2Kln(10z)]$where Uz (m s^{-1}) is the measured wind speed at height z (m) above the water surface (here at 2.5 m); C_{d10} is the drag coefficient at 10 m above the water surface (0.0013 m s^{-1}); and K is the von Karman constant (0.41). Wind speed was measured and recorded by an automatic meteorological station (Vantage Pro 2, China) installed at the MRE weather station, China Wetland Ecosystem Research Network.

2.4. Ebullitive CH$_4$ flux estimation

In order to estimate ebullitive CH$_4$ flux from the aquaculture ponds, the total CH$_4$ fluxes across the water-atmosphere interface were measured using the floating chamber method. On each sampling day, three plastic *FCs* were deployed on one transect spanning across Zones N, F, and A in each pond (Fig. 1c). The *FCs* were similar to those used in previous studies (Chuang et al., 2017; Lorke et al., 2015; Natchimuthu et al., 2014, 2017). Briefly, the opaque *FC* covering an area of 0.1 m^2 with a volume of 5.2 L was made from plastic basin (polyethylene/plexiglas®) with floats at the sides, and covered with reflective aluminum foil to minimize internal heating by sunlight. A fan was installed inside the chamber to mix the headspace air during gas sampling. In each sampling location, four gas samples (approximately 50 mL each) were taken from the chamber air headspace at 15-minute intervals over a total duration of 45 min, and transferred into 100 mL pre-evacuated airtight gas sampling bags (Dalian Delin Gas Packing Co., Ltd., China). The CH$_4$ concentration in the gas samples were determined using a gas chromatograph (GC-2010, Shimadzu, Kyoto, Japan) within 24 h after sampling. The rates of CH$_4$ flux (mg m^{-2} h^{-1}) were calculated by the regression of CH$_4$ concentration against time (Yang et al., 2019a). If the plastic floating chambers showed distinct nonlinear increases in CH$_4$ concentration, it was considered that the CH$_4$ fluxes from both diffusion and ebullition were captured (e.g., Chuang et al., 2017; Keller and Stallard, 1994; Zhu et al., 2016). In the current study, all chambers showed distinct nonlinear increases in CH$_4$ concentration, with the chamber-based fluxes being substantially larger than the diffusive fluxes calculated based on the gas transfer coefficient method. Therefore, the ebullitive CH$_4$ flux from our ponds was estimated by deducting the diffusive flux determined by the gas transfer model from the total CH$_4$ flux measured by the *FCs* (Chuang et al., 2017; Xiao et al., 2017; Yang et al., 2019a).

2.5. Measurement of sediment CH$_4$ production rates

Sediment cores (~15 cm length) were collected from the three different zones in each pond in May/mid-June, August, and October, which represented the initial, middle, and final culture stages, respectively, in 2017. The sediment cores were collected using a steel sediment sampler (internal diameter of 5 cm), and placed into incubation chambers made of transparent

Plexiglas (inner diameter = 5 cm, height = 25 cm). All the sediment samples were stored in an ice box and transported back to the laboratory within 4 h. Considering that the dissolved oxygen concentrations of the surface sediment in aquaculture ponds were almost close to zero, the sediment CH_4 production rates were measured using the anoxic incubation method in a dark and shaking incubator (Inglett et al., 2012; Wassmann et al., 1998; Yang et al., 2018). Before the start of incubation, the chambers were purged with ultrapure nitrogen (N_2) gas for 5–8 min to create an anaerobic condition (Vizza et al., 2017; Wassmann et al., 1998). The incubation chambers were then incubated for 6 days at *in situ* temperatures. Approximately 5 mL of gas samples were collected from the chamber using a polypropylene syringe equipped with a three-way stopcock at two-day intervals over the incubation period. After gas sampling, 5 mL of N_2 gas was added back into the chamber to re-establish the ambient atmospheric pressure. CH_4 concentrations in the gas samples were analyzed using a gas chromatograph. Sediment CH_4 production rates [μg CH_4 g^{-1} (dry weight) day^{-1}] were calculated based on the rate of change in chamber headspace CH_4 concentrations over the incubation period (Wassmann et al., 1998). In the present study, the dry weight was calculated by multiplying the wet weight of incubation sediment sample by (1 - the moisture content of incubation sediment sample).

2.6. Measurement of ancillary data

During each sampling campaign, various parameters of surface water (e.g., water temperature, salinity, pH, and dissolved oxygen) were determined *in situ* at a depth of 20 cm at each site. Water temperature and pH were measured using a portable pH/mV/Temperature meter (IQ150, IQ Scientific Instruments, USA). Water salinity and dissolved oxygen (DO) were determined using a salinity meter (Eutech Instruments-Salt6, USA) and a multiparameter probe (550A YSI, USA), respectively. The detection limits for pH, salinity, and DO were 0.01, 0.1 ppt and 0.1 mg L^{-1}, respectively. The relative standard deviations of pH, salinity, and DO analyses were ≤ 1.0%, ≤ 1.0%, and ≤ 2.0%, respectively. Meteorological parameters (e.g., air temperature, atmospheric pressure, and precipitation) were obtained from the automatic meteorological station (Vantage Pro 2, China) at the MRE weather station. The precision levels of air temperature, atmospheric pressure, and precipitation measurements were ±0.2 °C, ±1.5 hPa, and ±0.4 mm min^{-1}, respectively.

Sediment pH and electrical conductivity (EC) were determined using a pH meter (Orion 868, USA) and an EC meter (2265FS, Spectrum Technologies Inc., Phoenix, AZ, USA), respectively, in a slurry with a sediment to water ratio of 1:2.5 (w/v). A subsample of sediment was freeze-dried, homogenized, and then grounded to a fine powder for the analysis of total carbon (TC), total nitrogen (TN), $N-NO_3^-$ and SO_4^{2-}. Sediment TC and TN was determined using an elemental analyser (Elementar Vario MAX CN, Germany). The concentrations of $N-NO_3^-$ and SO_4^{2-} were determined following the methods of Tu et al. (2010), and Chen and Sun (2020), respectively, using a flow injection analyser (Skalar Analytical SAN^{++}, Netherlands). The detection limits for TC and TN were 4 μg L^{-1} and 3 μg L^{-1}, respectively, and the measurement reproducibilities were ≦1.0% and ≦2.0%, respectively. The physico-chemical properties of the shrimp pond sediment in 2017 were measured from the sediment samples at 0–15 cm depth from the three different zones in each pond, while the sediment properties in 2018 were the averages at two sampling depths (0–5, and 5–15 cm) at each sampling site.

2.7. Statistical analyses

Data were tested for normality and homogeneity of variance. Log-transformation of data was conducted for ebullitive CH_4 fluxes and sediment physicochemical parameters when necessary prior to the analysis of variance (ANOVA). Two–way ANOVA was conducted to examine the effects of sampling zones (Zones N, F, and A), sampling time, and their interactions on ebullitive CH_4 fluxes (or sediment physicochemical parameters) in aquaculture ponds with sampling ponds being specified as a random variable. The differences in mean ebullitive CH_4 fluxes and environmental variables between 2017 and 2018 were also tested using the independent samples t-test. Spearman correlation analyses were conducted to estimate the relationships (1) between ebullitive CH_4 fluxes (or sediment CH_4 production rates) and the environmental variables, and (2) between ebullitive CH_4 fluxes and sediment CH_4 production rates. Principal component analysis (PCA) was also performed to analyze the relationships between the ebullitive CH_4 fluxes and environmental parameters at different culture stages. All statistical analyses were conducted using SPSS statistical software (v. 17.0, SPSS Inc., USA) at a significance level of 0.05. The results were presented as means ± 1 standard error. All statistical plots were generated using OriginPro 7.5 (OriginLab Corp. USA).

3. Results

3.1. Surface sediment characteristics and gas transfer velocities

The spatial variations in sediment physico-chemical variables across the different zones within the ponds over the study period were shown in Figs. 2 and S1a. Overall, the mean sediment TC (Fig. 2a) and TN (Fig. 2b) concentrations were significantly higher in Zone F than the other two zones ($p<0.01$; Table S1). In contrast, sediment SO_4^{2-} (Fig. 2c), N–NO_3^- (Fig. 2d) and EC (Fig. 2f) were lowest in Zone F, followed by Zone N and Zone A (ANOVA, $p<0.05$; Table S1). However, no significant difference in sediment pH (Fig. 2e) and temperature (Fig. S1a) was observed among the three zones (ANOVA, $p>0.05$; Table S1).
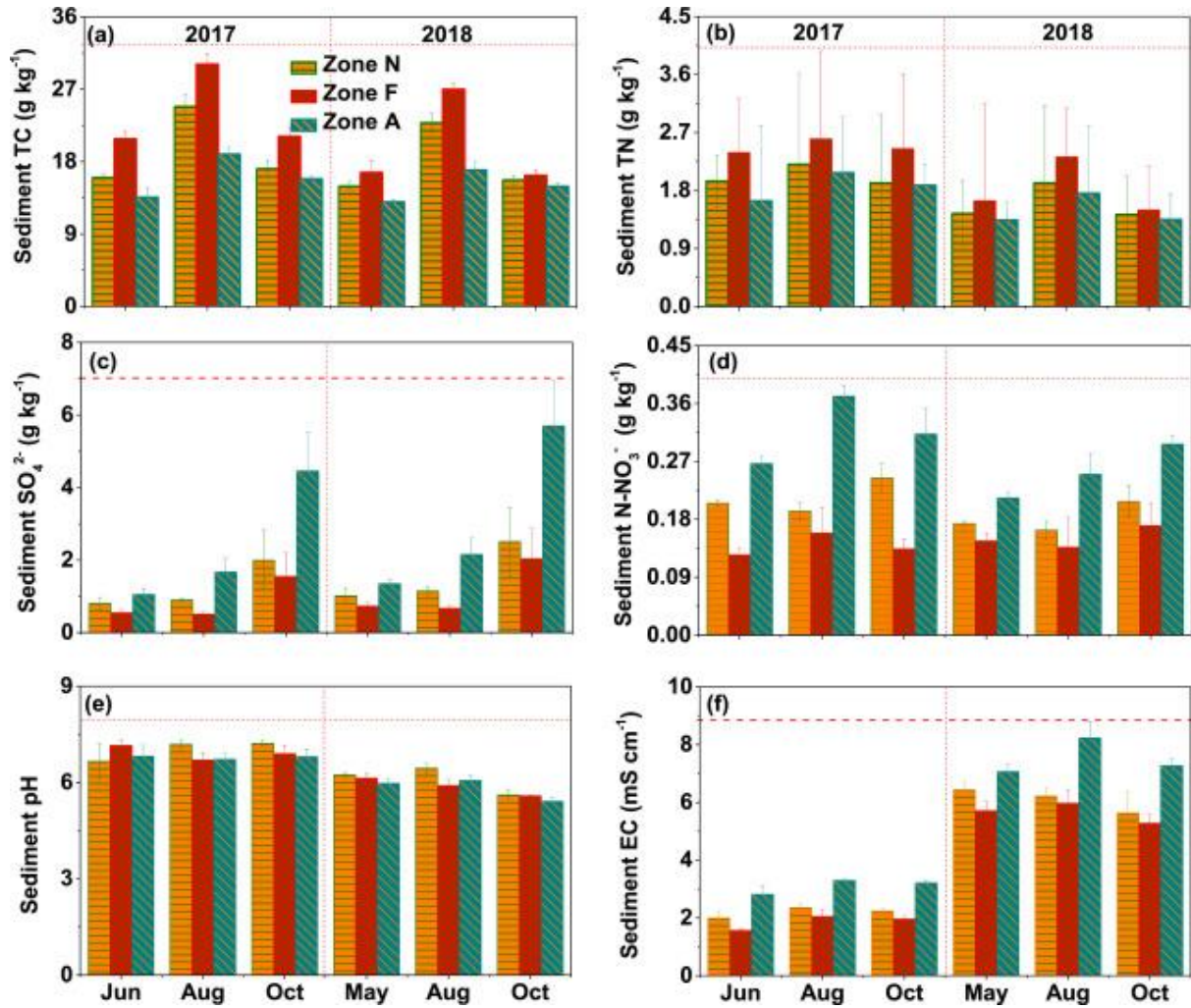
Fig. 2. Variations in (a) TC, (b) TN, (c) SO_4^{2-}, (d) $N-NO_3^-$, (e) pH, and (f) EC in the surface sediment (15 cm depth) in the three zones of aquaculture ponds in the Min River estuary during the aquaculture period. Zones N, F and A are nearshore area, feeding area and aeration area, respectively. Bars represent mean±1 SE ($n = 3$).

TC and TN exhibited similar temporal variations over the two years, with higher and lower concentrations being found at the middle (August) and initial stages (May or June), respectively (Fig. 2a and b). The sediment SO_4^{2-} content in the aquaculture ponds increased with time (Fig. 2c). The seasonal means of sediment TC, TN, $N–NO_3^-$ and pH in 2017 were slightly higher than those in 2018 ($p>0.05$), while the mean of sediment EC in 2017 was significantly lower than that in 2018 ($p<0.05$).

Gas transfer velocities (k_x) showed no clear seasonal patterns but varied significantly among measurement events (Fig. S1b). Across the sampling sites, k_x values ranged from 0.7 to 5.7 cm h^{-1} and from 0.5 to 3.0 cm h^{-1} in 2017 and 2018, respectively (Fig. S1b). The seasonal averages of k_x were 2.6±0.5 and 1.6±0.2 cm h^{-1} in 2017 and 2018, respectively.

3.2. Dissolved CH4 concentrations and sediment CH4 production rates

Dissolved CH_4 concentrations showed large spatiotemporal variations within the ponds. The average dissolved CH_4 concentrations during the aquaculture period ranged from 2.29±0.29 to 50.48±20.91 µM in 2017 (unpublished data), which were higher than those in 2018 (0.18±0.03−1.68±0.17 µM) (Fig. S2). In general, dissolved CH_4 concentrations were lowest in May/June, and highest in August/ September (Fig. S2). Over the two years, the mean dissolved CH_4 concentration was highest at Zone F (16.8 µM), followed by Zone N (4.2 µM) and Zone A (2.2 µM).

Sediment CH_4 production rates in the shrimp ponds ranged from 1.09 to 6.34 µg g^{-1} d^{-1} over the aquaculture period in 2017, which were higher than those in 2018 (0.03−0.53 µg g^{-1} d^{-1}, unpublished data). CH_4 production rates varied significantly among the three aquaculture stages in 2017 in the following descending order ($p<0.01$; Table 1): middle stage (August) > final stage (October) > initial stage (June) (Fig. 3). Among the three sampling zones, the highest and lowest CH_4 production rates were found in Zone F (2.51±0.25 – 5.64±0.63 µg g^{-1} d^{-1}) and Zone A (1.17±0.04 – 2.31±0.31 µg g^{-1} d^{-1}), respectively ($p<0.01$; Fig. 3; Table 1).

Table 1. Summary of two-way ANOVAs (with ponds ID specified as the random term) that examining the effect of sampling zones, sampling time (or stage) and their interactions on ebullitive CH_4 Flux (or sediment CH_4 production rates) at the aquaculture ponds in the Min River estuary.

| Fixed effect	Ebullitive CH_4 Flux					Sediment CH_4 production rates				
	Sum of squares	Mean square	df	F values	P values	Sum of squares	Mean square	df	F values	P values
Zones	21,776.744	10,888.372	2	43.678	0.002	19.332	9.666	2	270.856	<0.001
Time	115,379.591	3978.607	39	3.222	<0.001	22.655	11.328	2	21.990	0.007
Zones × Time	34,418.041	593.414	58	1.084	0.338	3.981	0.995	4	8.031	0.007
Residuals	98,495.369	547.196				5.324	0.296			
Random effect										
Ponds			2	0.331	0.720			2	2.494	0.246
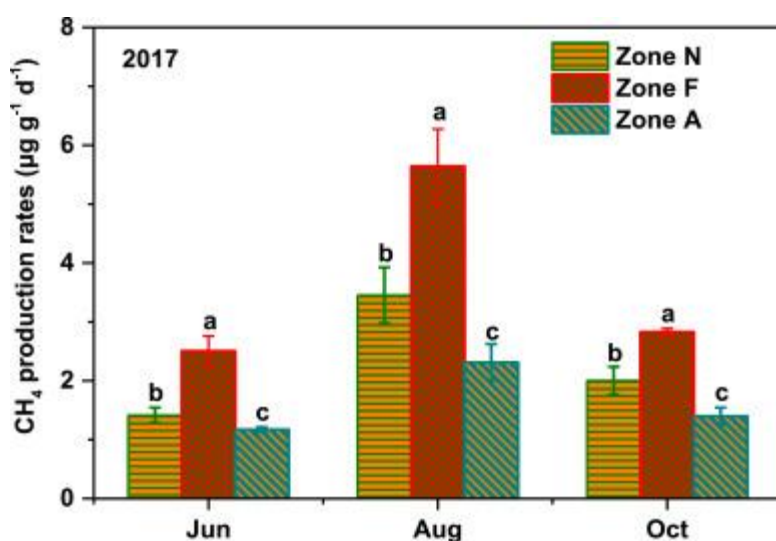
Fig. 3. Variations in sediment CH_4 production rates (0–15 cm depth) in the three zones of aquaculture ponds in the Min River estuary across the three aquaculture stages during the

aquaculture period in 2017. Zones N, F and A are nearshore area, feeding area and aeration area, respectively. Bars represent mean±1 SE ($n = 3$). Different lowercase letters above the bars indicate significant differences ($p<0.05$) between sampling zones during each culture stage.

3.3. Spatiotemporal variations in ebullitive CH₄ flux within ponds

Over the two years, ebullitive CH_4 fluxes differed significantly among the three zones within the ponds ($p<0.01$; Table 1), with the ranges of 0.17–77.14, 0.67–123.34, and 0.04–53.40 mg m^{-2} h^{-1} in Zones N, F and A, respectively (Fig. 4). When averaging the monthly fluxes, a strong spatial pattern in ebullitive CH_4 emissions emerged (Figure S3) with the rates decreasing in the order: Zone F > Zone N > Zone A.
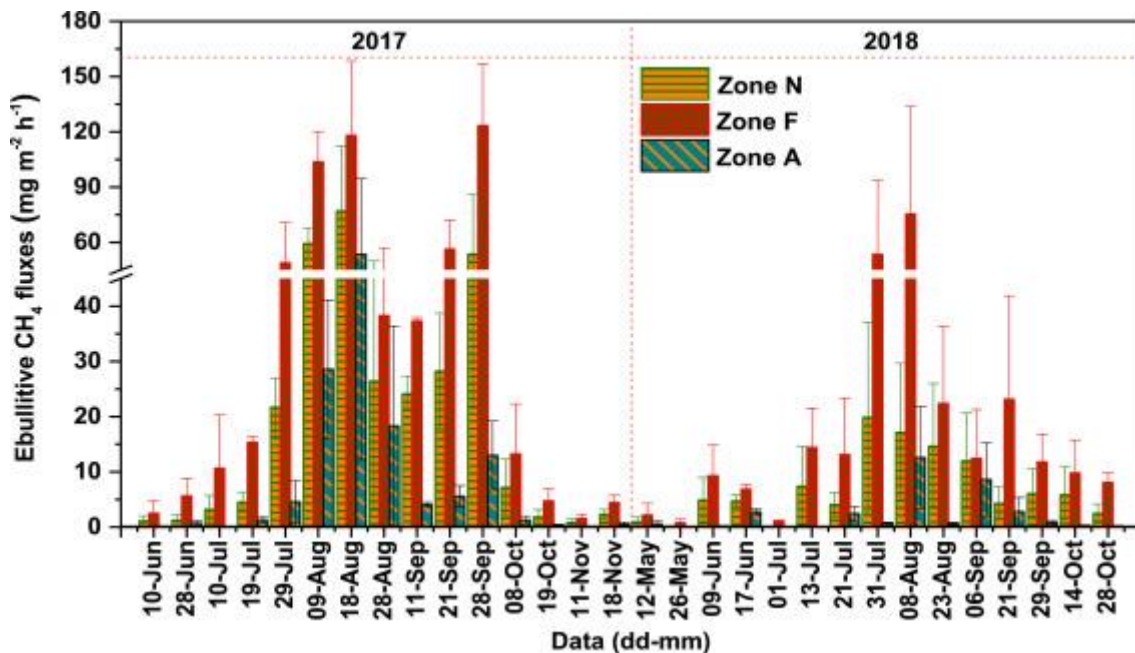

Fig. 4. Spatiotemporal variations in ebullitive CH_4 fluxes from aquaculture ponds in the Min River estuary during the aquaculture period. Zones N, F and A are nearshore area, feeding area and aeration area, respectively. Bars represent mean±1 SE ($n = 3$).

Ebullitive CH_4 fluxes also showed significant variations over time ($p<0.01$; Table 1), with lower fluxes in May/June and October/November, and higher fluxes in August/September (Fig. 4). Across all the sampling sites, the seasonal average of ebullitive CH_4 fluxes ranged from 0.85±0.04 to 82.89±18.90 mg m^{-2} h^{-1} over the aquaculture period in 2017, which was higher than those in 2018 (0.35±0.22 − 35.06±20.23 mg m^{-2} h^{-1}) ($p<0.01$).

3.4. Diffusive and ebullitive fluxes

During the aquaculture period in 2017, total CH_4 fluxes in Zones N, F, and A varied in the ranges of 1.16–78.75, 2.31–125.63, and 0.22–54.9 mg m^{-2} h^{-1}, respectively. On average, ebullition accounted for 95%, 97% and 88% of the total CH_4 emissions in Zones N, F, and A, respectively, with a minor contribution from diffusion (Fig. 5 and Table 2).
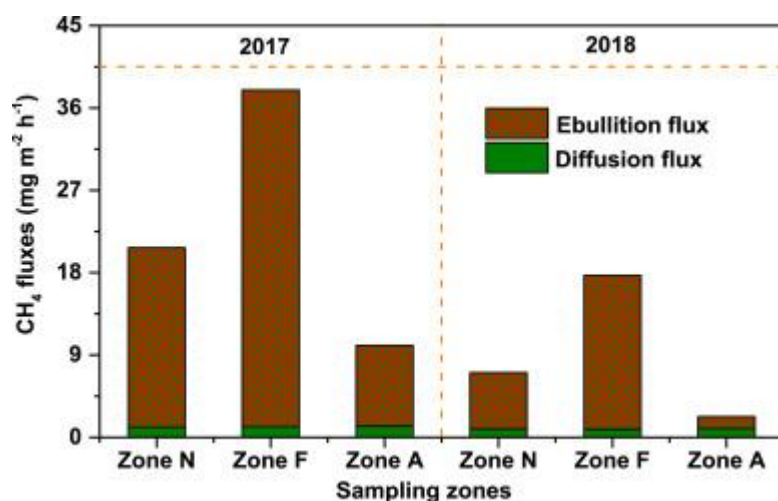
Fig. 5. CH₄ ebullition fluxes vs diffusion fluxes in the three zones of aquaculture ponds in the Min River estuary during the culture period in 2017 and 2018. Zones N, F, and A are nearshore area, feeding area, and aeration area, respectively.

Table 2. Contribution of ebullitive CH₄ fluxes to the total CH₄ fluxes (Mean ± SE, mg $m^{-2}\,h^{-1}$) across the different zones within ponds during the aquaculture period in 2017 and 2018. Zones N, F, and A are nearshore area, feeding area, and aeration area, respectively.

	2017				2018			
	Zone N	Zone F	Zone A	Average	Zone N	Zone F	Zone A	Average
Total fluxes	20.71±6.50	37.96±11.43	10.04±3.87	22.91±4.79	7.09±1.59	17.70±5.30	2.28±0.94	9.03±2.07
Ebullition fluxes	19.59±6.34	36.81±3.83	8.81±3.83	21.74±4.76	6.99±1.59	16.81±5.29	1.32±0.93	8.09±4.57
Contribution of Ebullition (%)	95	97	88	95	99	95	58	90

During the aquaculture period in 2018, total CH₄ fluxes also differed greatly among the three zones with the ranges of 0.25–19.92, 0.85–75.58, and 0.16–12.84 mg $m^{-2}\,h^{-1}$ in Zones N, F, and A, respectively. On average, ebullition accounted for 99%, 95% and 58% of the total CH₄ emissions in Zones N, F, and A, respectively (Fig. 5 and Table 2). When averaging the fluxes obtained at all sampling sites over the two years, ebullition contributed over 90% to the total CH₄ emission from ponds.

3.5. Relationships between ebullitive CH₄ flux and environmental variables

The results of Spearman correlation analysis showed that ebullitive CH₄ fluxes in the three zones of our ponds were positively correlated with sediment TC ($r=0.36-0.82$, $p<0.05$; Fig. S4) and TN content ($r=0.56-0.88$, $p<0.05$; Fig. S5), and negatively correlated with sediment SO_4^{2-} content ($r=0.41-0.78$, $p<0.05$; Fig. S6). Ebullitive CH₄ fluxes were also positively correlated with sediment CH₄ production rates across the sites on each sampling campaign ($r=0.58-0.85$, $p<0.01$; Fig. S7).

When data from the six sampling campaigns were analyzed together, ebullitive CH₄ fluxes were found to be positively correlated with sediment temperature ($r=0.49$, $p<0.01$), TC ($r=0.76$, $p<0.01$) and TN ($r=0.59$, $p<0.01$), and negatively correlated with water DO concentration ($r=-0.55$, $p<0.01$) and sediment SO_4^{2-} content ($r=-0.31$, $p<0.01$) (Table S2).

13

Our PCA results showed that the two principal components, i.e. PC1 and PC2, explained 95.6% and 3.7%, respectively, of the total variance in ebullitive CH_4 fluxes (Fig. 6). Ebullitive CH_4 efflux, sediment temperature, TC, TN and pH all displayed positive PC1 loading, while sediment SO_4^{2-}, $N-NO_3^-$ and EC showed negative PC1 loading (Fig. 6).
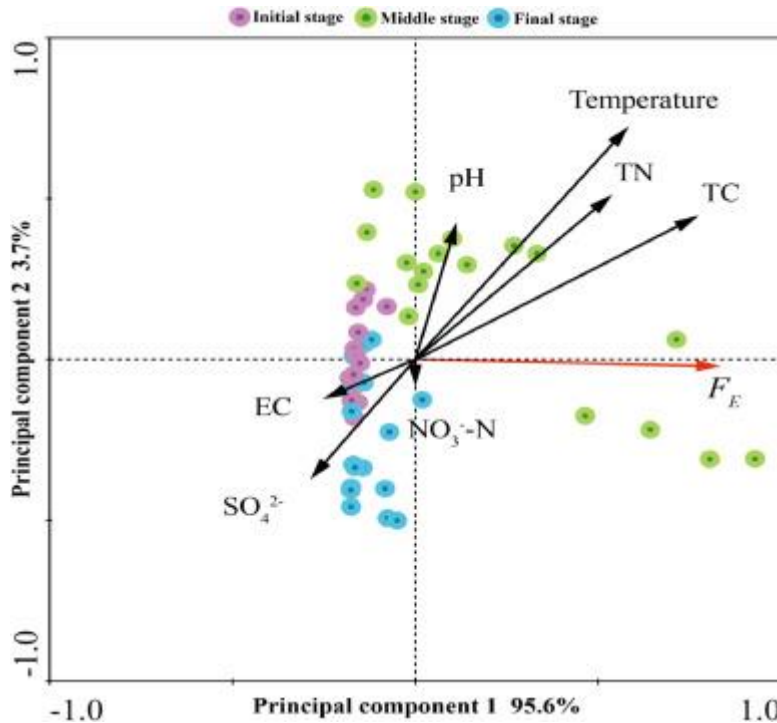

Fig. 6. The principal component analysis (PCA) biplots of the ebullitive CH_4 fluxes (F_E) and surface sediment characteristics of the aquaculture ponds, showing the loadings of environmental factors (arrows) and the scores of observations in three aquaculture stages (initial, middle and final stages).

4. Discussion

4.1. High CH_4 emissions largely attributed to ebullition

Previous studies have found that CH_4 ebullition plays a crucial role in influencing the magnitude of total CH_4 emissions from inland aquatic ecosystems (e.g., Bastviken et al., 2004, 2011; Wu et al., 2019; Zhu et al., 2016). The contributions of ebullition to total CH_4 emissions showed remarkable variations between different inland waters, ranging from 10% to 95% (e.g., Baulch et al., 2011; Deshmukh et al., 2016; Sawakuchi et al., 2014; Wu et al., 2019). For organic-rich shallow zones or freshwater systems, ebullitive fluxes were responsible for more than 50% of the total CH_4 emissions (e.g., Bastviken et al., 2008; Sawakuchi et al., 2014; Zhu et al., 2016). The extremely high CH_4 ebullitions from these aquatic systems are mainly attributed to the relatively shallow water depth and low hydrostatic pressure, which are more favorable for bubble formation and release in sediments (Casper et al., 2000; DelSontro et al., 2011; Zhu et al., 2016). Across the two years, the average total CH_4 emission (including both diffusive and ebullitive fluxes) from the shrimp ponds was 16.0 mg m^{-2} h^{-1}, which was equivalent to an annual emission of 69.5 g m^{-2} yr^{-1} (only considering the aquaculture period). Ebullitive fluxes were responsible for

more than 90% of the total CH_4 emissions over the two years. Both ebullitive CH_4 fluxes and total CH_4 emissions showed substantial inter-annual variations (Figs. 4 and 5), with lower rates in 2018 and higher values in 2017 (Table 2). Our results highlighted the significant contribution of ebullition to total CH_4 emissions from aquaculture ponds even in different years.

The total CH_4 flux in our estuarine mariculture ponds was lower than that reported in Lake Medo at the eastern Tibetan Plateau (Zhu et al., 2016), a eutrophic reservoir in Ohio, USA (Beaulieu et al., 2018), and the Gold Creek Reservoir in Australia (Sturm et al., 2014) (Table S3). However, the total CH_4 emission in our mariculture ponds was fairly comparable to the results in Lake Thimmapuram in south India (Attermeyer et al., 2016) and the Lixiahe River in southeast China (Wu et al., 2019). Moreover, the magnitude of total CH_4 fluxes in our ponds was one to two orders higher than that observed in various lakes in different climatic regions (e.g., Huttunen et al., 2001; Natchimuthu et al., 2016; Walter et al., 2008; Wik et al., 2013). The net CH_4 emission rates in our mariculture ponds were also substantially higher than those in a hydropower reservoir in Switzerland (Delsontro et al., 2010), several rivers in the Amazon (Sawakuchi et al., 2014), as well as many Chinese lakes (e.g., Chen et al., 2009a; Li et al., 2018; Wang et al., 2006; Xiao et al., 2017; Xing et al., 2005), reservoirs (e.g., Chen et al., 2009b; Li et al., 2018; Wang et al., 2017; Zhao et al., 2013; Zheng et al., 2011), and freshwater aquaculture ponds (e.g., Chen et al., 2016; Hu et al., 2014, 2016; Liu et al., 2015; Ma et al., 2018; Wu et al., 2018). In addition, the total CH_4 emission from our ponds during the aquaculture period was higher than the average of 1.4 mg m^{-2} h^{-1} in China's natural wetlands (Wei and Wang, 2017), and was approximately 6 times higher than the average of 2.6 mg m^{-2} h^{-1} in the *Cyperus malaccensis* marsh from an adjacent estuary (Yang et al., 2019b). As seen in Table S3, ebullitive fluxes generally accounted for more than 80% of the total CH_4 emission in most aquatic ecosystems. Hence, the much higher total CH_4 fluxes observed in our mariculture ponds, compared to many other aquatic ecosystems, might imply the presence of a considerably high rate of CH_4 ebullition.

4.2. Feeding areas as hotspots of ebullitive CH_4 emission

Ebullitive CH_4 emission in aquaculture ponds at a high spatial resolution remains poorly characterized. As the first attempt to investigate the fine-scale spatial variations in CH_4 ebullition in aquaculture ponds, this study showed that the mean ebullitive CH_4 efflux at Zone F was higher than those in Zones A and N by over 5 and 2 times, respectively (Fig. S3 and Table 2). Our results highlighted the strong spatial variations in ebullitive CH_4 emission within the ponds, with the feeding areas being the ebullition hotspot areas. The extremely high rate of CH_4 ebullition in Zone F could be primarily ascribed to the large organic matter loading in sediment that enhanced CH_4 production. Over the two-year period, the mean sediment TC concentration in Zone F was higher than those in Zones N and A by 12–24% and 33–49%, respectively. Mean sediment TN concentration in Zone F was also higher than those in Zones N and A by 14–23% and 23–33%, respectively. Previous studies have shown that CH_4 in aquatic ecosystems is mainly generated from the organic-rich sediments (e.g., Bastviken et al., 2008; Grinham et al., 2018b; Xiao et al., 2017; Zhou et al., 2019). Organic matter in sediments provides the key carbon substrates for methanogenic activities, thereby providing favorable conditions for CH_4 production and bubble formation (Bastviken et al., 2008; Davidson et al., 2018; Walter et al., 2008; Zhu et al., 2016). The higher sediment organic C and N loads in Zone F would have contributed to larger CH_4 production (Fig. 3), and consequently larger CH_4 ebullition as compared to Zones A and

N. This was further confirmed by the significant and positive relationships observed (1) between ebullitive CH_4 fluxes and sediment CH_4 production rates (Fig. S7), and (2) between ebullitive CH_4 fluxes (or sediment CH_4 production rates) with sediment TC (Table S2, Fig. S4 and Fig. S8b) and TN (Table S2 and Fig. S5) concentrations.

Net CH_4 release from the aquatic systems to the atmosphere is determined by the processes of CH_4 production by methanogens, CH_4 oxidation by methanotrophs, and CH_4 transport. CH_4 oxidation can effectively reduce net CH_4 emissions to the atmosphere (Bastviken et al., 2008), and is governed by the DO level in the water column (Sundh et al., 2005; Yang et al., 2019b). CH_4 oxidation rates in the water column have been found to increase with the concentrations of dissolved CH_4 and DO (Bastviken et al., 2008; Matoušů et al., 2017; Yang et al., 2019c). Aquaculture ponds are aerated on a daily basis in Zone A (Yang et al., 2019a), which can improve the oxygen supply to the sediment surface and reduce the development of anaerobic conditions, ultimately leading to an inhibition of CH_4 production but an enhancement of CH_4 oxidation (Liu et al., 2015; Schrier-Uijl et al., 2011; Yang et al., 2019a). Although CH_4 oxidation rates in the present study were unavailable, our observation of the significant and negative relationship between sediment CH_4 production rates and water DO concentrations ($r=0.70$, $p<0.01$; Table S2) supported the influence of oxygen on methanogenesis. Furthermore, the aeration-induced physical disturbance of pond water might lead to the burst of CH_4 bubbles, which in turn promote the oxidation of a large proportion of the produced CH_4 in the water column before its release into the atmosphere. Therefore, aeration activity was considered as an important contributor to the lower ebullitive CH_4 fluxes detected in Zone A.

4.3. Temporal variations in ebullitive CH_4 fluxes

Ebullitive CH_4 flux has been reported to vary temporally in inland waters (e.g., Natchimuthu et al., 2014; Wik et al., 2013; Wu et al., 2019). In our study, ebullitive CH_4 emissions from the estuarine aquaculture ponds also showed considerable variations between different seasons (Fig. 4 and Table 1). The seasonal mean ebullitive CH_4 emissions in 2017 were positively correlated with sediment CH_4 production rates (0–15 cm depth) ($r=0.79$, $p<0.01$). As such, the seasonal patterns of ebullitive CH_4 emissions were largely similar to those of sediment CH_4 production rates (0–15 cm depth) (Fig. 3). A high CH_4 production rate in sediments would increase the CH_4 concentrations in sediment porewater and subsequently the production and release of CH_4 bubbles to the atmosphere. Previous studies found that the seasonal patterns of CH_4 metabolism are governed by seasonal variations in temperature which drive the production of substrate precursors and microbial activity (Crawford et al., 2014; Rosentreter et al., 2017; Vizza et al., 2017). Our Spearman correlation (Table S2) and PCA (Fig. 6) results suggested that the seasonal pattern of ebullitive CH_4 fluxes (or CH_4 sediment production rates) generally followed the patterns of sediment temperature, TC and TN, but were opposite to the pattern of sediment SO_4^{2-}. Therefore, the lower ebullitve CH_4 fluxes in the initial and final stages of aquaculture were primarily ascribed to low organic matter availability, high SO_4^{2-} in sediments and low water temperature, which reduced the substrate availability and metabolic activity of methanogens (Kelly and Chynoweth, 1981; Sun et al., 2013; Vizza et al., 2017). In contrast, high ebullitive CH_4 emissions observed in the middle stages of aquaculture were influenced, to a large extent, by the interactions between high sediment temperature, large organic matter load, and low sediment SO_4^{2-} content, which favored methanogenic activities (Davidson et al., 2018; Sun et al., 2013; Vizza et al., 2017). Further studies should be done to explore the exact

effects of microbial abundance and activity on CH_4 production and emission in aquaculture ponds.

We also observed substantial interannual variations in ebullitive CH_4 fluxes in this study (Fig. 4 and Table 2). The mean ebullitive CH_4 flux over the whole aquaculture period was 21.74 ± 4.76 mg m^{-2} h^{-1} in 2017, which was significantly higher than that in 2018 (8.09 ± 4.57 mg m^{-2} h^{-1}) ($p<0.01$; Table 2). The interannual variations in ebullitive CH_4 emissions from the aquaculture ponds could possibly be ascribed to the variations in mean sediment temperature (25.0 °C in 2017 vs 22.9 °C in 2018), TC (19.8 vs 17.5 g kg^{-1}), and TN (2.1 vs 1.6 g kg^{-1}) between the two years, which was in line with the previous discussion regarding the effect of temperature and substrate availability on CH_4 metabolism. Furthermore, the mean sediment SO_4^{2-} content (1.4 g kg^{-1}) and EC (2.4 mS cm^{-1}) over the aquaculture period in 2017 were much lower than those in 2018 (SO_4^{2-}: 1.9 g kg^{-1}; EC: 6.4 mS cm^{-1}), as a result of freshwater dilution caused by the combination of high precipitation and large surface runoff. High salinity has been shown to support sulfate reduction that could lead to enhanced anaerobic CH_4 oxidation in sediments and intensified competition between sulfate reducing bacteria and methanogens (Chambers et al., 2013; van der Gon et al., 2001; Vizza et al., 2017). Subsequently, CH_4 fluxes decreased with the increase of SO_4^{2-} and salinity levels, as reported in coastal wetlands (Poffenbarger et al., 2011; Vizza et al., 2017; Wilson et al., 2015) and waters (Welti et al., 2017; Yang et al., 2018). The much lower sediment SO_4^{2-} content and salinity in 2017 (Fig. 2c and f) could have promoted methanogenic activities markedly, as supported by the higher sediment CH_4 production rates in 2017 than in 2018 (1.09–6.34 vs 0.03–0.53 µg g^{-1} d^{-1}), which in turn enhanced CH_4 ebullition.

4.4. Implications for ebullitive CH_4 flux from aquaculture ponds

The seasonal integrated ebullitive CH_4 fluxes from the aquaculture ponds during the culture period in 2017 and 2018 were found to be 0.4–40.4 g CH_4 m^{-2} in Zone N, 1.1–64.5 g CH_4 m^{-2} in Zone F, and 0.2–24.9 g CH_4 m^{-2} in Zone A. In our ponds, Zones A, F and N covered 65%, 25%, and 10% of the total surface area, respectively. Zones F and N had a disproportionately high impact on CH_4 ebullition, contributing to 49.7–71.8% and 20.1–33.6% of the spatially averaged ebullitive fluxes (Fig. 7). Our results highlighted the importance of considering the spatial variations in ebullitive CH_4 emission within ponds during the upscaling of small-scale CH_4 fluxes to the whole pond level (Fig. 7).
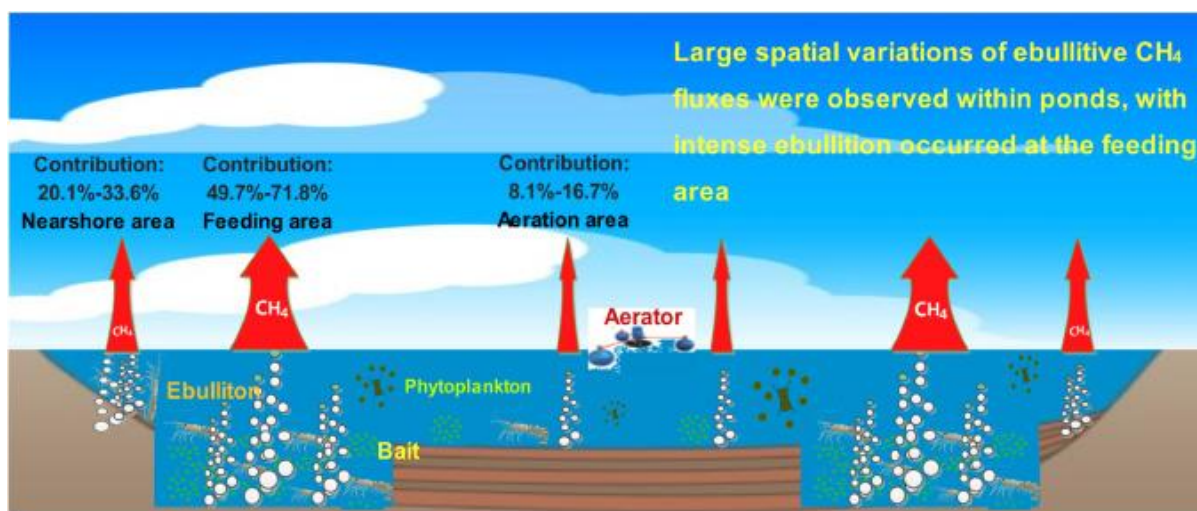
Fig. 7. Conceptual diagram illustrating the spatial variations in ebullitive CH_4 fluxes within aquaculture pond during the aquaculture period.

Due to the growing global demand for seafood, an increasing number of aquaculture ponds have been built and the total area of aquaculture ponds has increased continually over the last decades in the coastal areas in China and many other countries (Ren et al., 2019; Yang et al., 2020a). Thus, it is an imminent challenge to balance seafood production and greenhouse gas mitigation for the sustainable development of aquaculture sector (Yang, 2014). Our results indicated that high ebullitive CH_4 emission occurred in the feeding zone with high residue bait accumulation, while low CH_4 fluxes were maintained at the aeration zone (Fig. S3 and Fig. 7). Given the observed large within-pond variations in CH_4 flux, reducing the built-up of unconsumed feeds and increasing aeration are important strategies for mitigating CH_4 emissions from the mariculture ponds.

Some efforts have been made to estimate large-scale CH_4 emissions from aquaculture systems by extrapolating short-term field measurements (< 1 year) to longer periods in a given area (e.g., Hu et al., 2016; Yang et al., 2018; Yuan et al., 2019). However, our results showed that ebullitive CH_4 emissions from the estuarine aquaculture ponds had strong inter-annual variation, with the average fluxes differing by more than two-fold between the two years, which implied a large uncertainty of CH_4 flux estimation based on short-term measurements. Therefore, it is crucial to make long-term observations in order to minimize the potential bias of CH_4 flux estimates and improve our understanding of CH_4 budget. Furthermore, ebullitive CH_4 emissions from the estuarine aquaculture ponds varied considerably between different months (Fig. 4), with the coefficients of variation ranging between 110%–117%. These findings indicated the potential problem of extrapolating flux estimates from a single month to seasonal or annual scales, exacerbating the uncertainty of CH_4 emission estimates. Therefore, it is suggested that flux measurements should be conducted in as many sites as practicable over multiple months in order to achieve a more accurate CH_4 flux estimate and enhance our understanding of CH_4 dynamics in aquaculture ponds.

4.5. Limitation and future research

Similar to many studies, there are some limitations in the current study. First, ebullitive CH_4 fluxes were determined in the aquaculture ponds in MRE, southeast China only. Care

should be taken in upscaling our ebullitive CH_4 fluxes to broader spatial scales. To further improve the accuracy of estimates of regional or global ebullitive CH_4 emissions from mariculture ponds, more works on the effects of other factors, such as regional climate, aquaculture types, and management practice, on CH_4 flux are needed. Second, while sediment TC and TN were analyzed in the current study, other chemical and biological variables, such as autochthonous and allochthonous dissolved organic matter (Zhou et al., 2019), and the abundance and activity of methanogens and methanotrophs, can also influence the spatiotemporal variations in ebullitive CH_4 emission in aquatic ecosystems. Therefore, future studies should further explore the influence of a wider range of physio-chemical and biological variables on CH_4 ebullition. Third, previous studies have shown that CH_4 ebullition events were often coincided with low atmospheric pressure (Mattson and Likens, 1990; Tokida et al., 2007; Zhu et al., 2016). Tropical cyclones are extreme perturbations that can cause a rapid drop in atmospheric pressure, which in turn can trigger substantial CH_4 ebullition in tropical coastal areas. Therefore, more direct measurement of CH_4 ebullition should be done during the period of typhoon passage in coastal mariculture ponds (Yang et al., 2020b). Fourth, direct measurement of the diel pattern of ebullitive CH_4 fluxes was unavailable in the current study, although diurnal variations in CH_4 emission have been reported in lakes (e.g., Erkkilä et al., 2018; Hirota et al., 2007; Xing et al., 2004). Future research should quantify the diel variations in ebullitive CH_4 fluxes from aquaculture ponds. Fifth, our floating chambers might fail to completely capture all the ebullition events, leading to a gross under-estimation of annual CH_4 emission. In future, more advanced measurement techniques should be applied to more accurately measure the ebullitive CH_4 emission from aquaculture ponds. Lastly, our study did not consider the influence of water velocity in the estimation of diffusive CH_4 fluxes from the aquaculture ponds. A gas transfer coefficient model that consider both wind speed and water velocity could be used in further studies to improve the accuracy of diffusive CH_4 flux estimates in aquatic ecosystems.

5. Conclusions

This study was the first to characterize the spatiotemporal variations in ebullitive CH_4 fluxes within aquaculture ponds. Our results showed that ebullitive CH_4 emissions contributed to over 90% of the total CH_4 emission from aquaculture ponds, indicating the importance of ebullition in transporting CH_4 from the ponds to the atmosphere. Ebullitive CH_4 fluxes varied significantly between the two measurement years and within the ponds. Intense CH_4 ebullition from the ponds occurred in the middle stage of aquaculture (July to September), which could be attributed to the large organic matter loading and high temperature during this period in the subtropical estuarine environment. The feeding area was a hotspot of CH_4 ebullition, contributing 49.7–71.8% to the spatially averaged ebullitive fluxes. Our results showed that flux measurements based on a single point in space or time would introduce marked biases in estimating whole-pond ebullitive CH_4 emissions. Field measurements of CH_4 ebullition should be done in as many sites as practicable over a longer term in order to produce more accurate estimates of ebullitive CH_4 fluxes at the whole-pond or even larger scales.

Acknowledgments

References

Attermeyer, K., Flury, S., Jayakumar, R., Fiener, P., Steger, K., Arya, V., Wilken, F., Van Geldern, R., Premke, K., 2016. Invasive floating macrophytes reduce greenhouse gas emissions from a small tropical lake. Sci. Rep. 6, 1–10. https://doi.org/10. 1038/srep20424 .

Avnimelech, Y., Ritvo, G., 2003. Shrimp and fish pond soils: processes and management. Aquaculture 220, 549–567. https://doi.org/10.1016/S0044-8486(02) 00641-5.

Bastviken, D., Cole, J., Pace, M., Tranvik, L., 2004. Methane emissions from lakes: dependence of lake characteristics, two regional assessments, and a global estimate. Global Biogeochem. Cy. 18. GB4009 https://doi.org/10.1029/ 20 04GB0 02238 .

Bastviken, D., Cole, J.J., Pace, M.L., Van de Bogert, M.C., 2008. Fates of methane from different lake habitats: connecting whole-lake budgets and CH 4 emissions. J. Geophys. Res. 113, G02024. https://doi.org/10.1029/20 07JG0 0 0608 .

Bastviken, D., Sundgren, I., Natchimuthu, S., Reyier, H., Gålfalk, M., 2015. Cost- efficient approaches to measure carbon dioxide (CO 2) fluxes and concentrations in terrestrial and aquatic environments using mini loggers. Biogeosciences 12 (12), 3849–3859. https://doi.org/10.5194/bg- 12- 3849- 2015 .

Bastviken, D., Tranvik, L.J., Downing, J.A., Crill, P.M., Enrich-Prast, A., 2011. Freshwater methane emissions offset the continental carbon sink. Science 331, 50. https: //doi.org/10.1126/science.1196808 .

Baulch, H.M., Dillon, P.J., Maranger, R., Schiff, S.L., 2011. Diffusive and ebullitive transport of methane and nitrous oxide from streams: are bubble- mediated fluxes important? J. Geophys. Res. 116 (G4). https://doi.org/10.1029/ 2011JG001656 .

Beaulieu, J.J., Balz, D.A., Birchfield, M.K., Harrison, J.A., Nietch, C.T., Platz, M.C., Squier, W.C., Waldo, S., Walker, J.T., White, K.M., 2018. Effects of an experimental water-level drawdown on methane emissions from a eutrophic reservoir. Ecosystems 21 (4), 657–674. https://doi.org/10.1007/s10021- 017- 0176- 2 .

Bogard, M.J., del Giorgio, P.A., Boutet, L., Chaves, M.C.G., Prairie, Y.T., Merante, A., Derry, A.M., 2014. Oxic water column methanogenesis as a major component of aquatic CH 4 fluxes. Nat. Commun. 5, 5350. https://doi.org/10.1038/ncomms6350 .

Borges, A.V., Darchambeau, F., Teodoru, C.R., Marwick, T.R., Tamooh, F., Geeraert, N., Omengo, F.O., Guérin, F., Lambert, T., Morana, C., Okuku, E., Bouillon, S., 2015. Globally significant greenhouse gas emissions from African inland waters. Nat. Geosci. 8 (8), 637–642. https://doi.org/10.1038/NGEO2486 .

Borges, A.V., Darchambeau, F., Lambert, T., Bouillon, S., Morana, C., Brouyère, S., Hakoun, V., Jurado, A., Tseng, H.-C., Descy, J.-P., Roland, F.A.E., 2018. Effects of agricultural land use on fluvial carbon dioxide, methane and nitrous oxide concentrations in a large European river, the Meuse (Belgium). Sci. Total Environ. 610- 611, 342–355. http://dx.doi.org/10.1016/j.scitotenv.2017.08.047 .

Bureau of Fisheries of the Ministry of Agriculture, 2019. China Fishery Statistics Yearbook. China Agriculture Press, Beijing (in Chinese) . van Bergen, T.J.H.M., Barros, N., Mendonça, R., Aben, R.C.H., Althuizen, I.H.J., Huszar, V., Lamers, L.P.M., Lürling, M., Roland, F., Kosten, S., 2019. Seasonal and diel variation in greenhouse gas emissions from an urban pond and its major drivers. Limnol. Oceanogr. 64 (5), 2129–2139. https://doi.org/10.1002/lno.11173 .

Cao, L., Wang, W., Yang, Y., Yang, C., Yuan, Z., Xiong, S., Diana, J., 2007. Environmental impact of aquaculture and countermeasures to aquaculture pollution in China. Environ. Sci. Pollut. R. 14 (7), 452–462. https://doi.org/10.1065/espr2007.05.426 .

Casper, P. , Maberly, S.C. , Hall, G.H. , Finlay, B.J. , 2000. Fluxes of methane and carbon dioxide from a small productive lake to the atmosphere. Biogeochemistry 49 (1), 1–19 .

Chambers, L.G., Osborne, T.Z., Reddy, K.R., 2013. Effect of salinity-altering pulsing events on soil organic carbon loss along an intertidal wetland gradient: a laboratory experiment. Biogeochemistry 115 (1-3), 363–383. https://doi.org/10.1007/ s10533- 013- 9841- 5 .

Chen, Y., Dong, S.L., Wang, Z.N., Wang, F., Gao, Q.F., Tian, X.L., Xiong, Y.H., 2015. Variations in CO_2 fluxes from grass carp *Ctenopharyngodon idella* aquaculture polyculture ponds. Aquacult. Environ. Interac. 8, 31–40. https://doi.org/10.3354/ aei00149 .

Chen, B.B., Sun, Z.G., 2020. Effects of nitrogen enrichment on variations of sulfur in plant-soil system of Suaeda salsa in coastal marsh of the Yellow River estuary. China. Ecol. Indic. 109, 105797. https://doi.org/10.1016/j.ecolind.2019.105797 .

Chen, H., Wu, N., Yao, S., Gao, Y., Zhu, D., Wang, Y., Xiong, W., Yuan, X., 2009a. High methane emissions from a littoral zone on the Qinghai-Tibetan plateau. Atmos. Environ. 43 (32), 4995–50 0 0. https://doi.org/10.1016/j.atmosenv.20 09.07.0 01 .

Chen, H., Wu, Y., Yuan, X., Gao, Y., Wu, N., Zhu, D., 2009b. Methane emissions from newly created marshes in the drawdown area of the Three Gorges Reservoir. J. Geophys. Res. 114, D18301. https://doi.org/10.1029/2009JD012410 .

Chen, Y., Dong, S.L., Wang, F., Gao, Q.F., Tian, X.L., 2016. Carbon dioxide and methane fluxes from feeding and no-feeding mariculture ponds. Environ. Pollut. 212, 4 89–4 97. http://dx.doi.org/10.1016/j.envpol.2016.02.039 .

Chuang, P.-C., Young, M.B., Dale, A.W., Miller, L.G., Herrera-Silveira, J.A., Paytan, A., 2017. Methane fluxes from tropical coastal lagoons surrounded by mangroves, Yucatán, Mexico. J. Geophys. Res. Biogeosci. 122 (5), 1156–1174. http://dx.doi. org/10.10 02/2017JG0 03761 .

Cole, J.J. , Caraco, N.F. , 1998. Atmospheric exchange of carbon dioxide in a low-wind oligotrophic lake measured by the addition of SF6. Limnol. Oceanogr. 43 (4), 647–656 .

Cotovicz Jr., L.C., Knoppers, B.A., Brandini, N., Poirier, D., Costa Santos, S.J., Abril, G., 2016. Spatio-temporal variability of methane (CH4) concentrations and diffusive fluxes from a tropical coastal embayment surrounded by a large urban area (Guanabara Bay, Rio de Janeiro, Brazil). Limnol. Oceanogr 61 (S1), S238–S252. https://doi.org/10.1002/lno.10298 .

Crawford, J.T., Stanley, E.H., Spawn, S.A., Finlay, J.C., Loken, L.C., Striegl, R.G., 2014. Ebullitive methane emissions from oxygenated wetland streams. Glob. Change Biol. 20 (11), 3408–3422. https://doi.org/10.1111/gcb.12614 .

Davidson, T.A., Audet, J., Jeppesen, E., Landkildehus, F., Lauridsen, T.L., Søndergaard, M., Syväranta, J., 2018. Synergy between nutrients and warming enhances methane ebullition from experimental lakes. Nat. Clim. Change 8 (2), 156. https://doi.org/10.1038/s41558- 017- 0063- z .

DelSontro, T., Kunz, M.J., Kempter, T., Wüest, A., Wehrli, B., Senn, D.B., 2011. Spatial heterogeneity of methane ebullition in a large tropical reservoir. Environ. Sci. Technol. 45, 9866–9873. https://doi.org/10.1021/es2005545 .

Delsontro, T., McGinnis, D.F., Sobek, S., Ostrovsky, I., Wehrli, B., 2010. Extreme methane emissions from a Swiss hydropower reservoir: contribution from bub- bling sediments. Environ. Sci. Technol. 44 (7), 2419–2425. https://doi.org/10. 1021/es9031369 .

Deshmukh, C., Guérin, F., Labat, D., Pighini, S., Vongkhamsao, A., Guédant, P., Rode, W., Godon, A., Chanudet, V., Descloux, S., Serça, D., 2016. Low methane (CH 4) emissions downstream of a monomictic subtropical hydroelectric reser- voir (Nam Theun 2, Lao PDR). Biogeosciences 13 (6), 1919–1932. https://doi.org/ 10.5194/bg- 13- 1919- 2016 .

Erkkilä, K.M., Ojala, A., Bastviken, D., Biermann, T., Heiskanen, J.J., Lindroth, A., et al., 2018. Methane and carbon dioxide fluxes over a lake: comparison between eddy covariance, floating chambers and boundary layer method. Biogeosciences 15 (2), 429–445. https://doi.org/10.5194/bg-15-429-2018 .

Gålfalk, M. , Olofsson, G. , Crill, P. , Bastviken, D. , 2016. Making methane visible. Nat. Clim. Change 6, 426–430 . Gorsky, A.L., Racanelli, G.A., Belvin, A.C., Chambers, R.M., 2019. Greenhouse gas flux from stormwater ponds in southeastern Virginia (USA). Anthropocene, 100218. https://doi.org/10.1016/j.ancene.2019.100218 .

Grinham, A., Albert, S., Deering, N., Dunbabin, M., Bastviken, D., Sherman, B., Love- lock, C.E., Evans, C.D., 2018a. The importance of small artificial water bodies as sources of methane emissions in Queensland, Australia. Hydrol. Earth Syst. Sci. 22, 5281–5298. https://doi.org/10.5194/hess- 22- 5281- 2018 .

Grinham, A., Dunbabin, M., Albert, S., 2018b. Importance of sediment organic matter to methane ebullition in a sub-tropical freshwater reservoir. Sci. Total Environ. 621, 1199–1207. https://doi.org/10.1016/j.scitotenv.2017.10.108 .

Grinham, A., Dunbabin, M., Gale, D., Udy, J., 2011. Quantification of ebullitive and diffusive methane release to atmosphere from a water storage. Atmos. Environ. 45 (39), 7166–7173. https://doi.org/10.1016/j.atmosenv.2011.09.011 .

van der Gon, H.A.D. , van Bodegom, P.M. , Wassmann, R. , Lantin, R.S. , Metra-Cor- ton, T.M. , 2001. Sulfate-containing amendments to reduce methane emissions from rice fields: mechanisms, effectiveness and costs. Mitig. Adaptat. Strat. Gl. 6, 71–89 .

Hamilton, J.D., Kelly, C.A., Rudd, J.W.M., Hesslein, R.H., Roulet, N.T., 1994. Flux to the atmosphere of CH_4 and CO_2 from wetland ponds on the Hudson Bay low- lands (HBLs). J. Geophys. Res.-Atmos. 99, 1495–1510. https://doi.org/10.1029/ 93JD03020 .

Herbeck, L.S., Unger, D., Wu, Y., Jennerjahn, T.C., 2013. Effluent, nutrient and organic matter export from shrimp and fish ponds causing eutrophication in coastal and back-reef waters of NE Hainan, tropical China. Cont. Shelf Res. 57, 92–104. http://dx.doi.org/10.1016/j.csr.2012.05.006 .

Hirota, M., Senga, Y., Seike, Y., Nohara, S., Kunii, H., 2007. Fluxes of carbon dioxide, methane and nitrous oxide in two contrastive fringing zones of coastal lagoon, Lake Nakaumi, Japan. Chemosphere 68 (3), 597–603. https://doi.org/10.1016/j. chemosphere.20 07.01.0 02 .

Holgerson, M.A., 2015. Drivers of carbon dioxide and methane supersaturation in small, temporary ponds. Biogeochemistry 124 (1-3), 305–318. https://doi.org/10. 1007/s10533-015-0099-y .

Holgerson, M.A., Raymond, P.A., 2016. Large contribution to inland water CO_2 and CH_4 emissions from very small ponds. Nat. Geosci. 9 (3), 222–226. https://doi. org/10.1038/NGEO2654 .

Hu, B.B., Wang, D.Q., Zhou, J., Meng, W.Q., Li, C.W., Sun, Z.B., Guo, X., Wang, Z.L., 2018. Greenhouse gases emission from the sewage draining rivers. Sci. Total Environ. 612, 1454–1462. https://doi.org/10.1016/j.scitotenv.2017.08.055 .

Hu, Z., Lee, J.W., Chandran, K., Kim, S., Sharma, K., Khanal, S.K., 2014. Influence of carbohydrate addition on nitrogen transformations and greenhouse gas emissions of intensive aquaculture system. Sci. Total. Environ. 470, 193–200. https: //doi.org/10.1016/j.scitotenv.2013.09.050 .

Hu, Z.Q. , Wu, S. , Ji, C. , Zou, J.W. , Zhou, Q.S. , Liu, S.W. ,2016. A comparison of methane emissions following rice paddies conversion to crab-fish farming wetlands in southeast China. Environ. Sci. Pollut. Res. 23 (2), 1505–1515 https://doi.org/0.1007/s11356-015-5383-9 .

Huttunen, J.T., Lappalainen, K.M., Saarijärvi, E., Väisänen, T., Martikainen, P.J., 2001. A novel sediment gas sampler and a subsurface gas collector used for measurement of the ebullition of methane and carbon dioxide from aeutrophied lake. Sci. Total Environ. 266 (1), 153–158. https://doi.org/10.1016/S0048-9697 .

Inglett, K.S. , Inglett, P.W. , Reddy, K.R. , Osborne, T.Z. , 2012. Temperature sensitivity of greenhouse gas production in wetland soils of different vegetation. Biogeochemistry 108, 77–90 .

IPCC, 2013. Climate Change 2013: The Physical Science Basis. In: Stocker, T.F. (Ed.), Contribution of Working Group I to the Fifth Assessment Report of the Inter- governmental Panel on Climate Change. Cambridge Univ. Press and others [eds.] https://doi.org/10.1017/CBO9781107415324 .

IPCC, 2019. In: Calvo Buendia, E., Tanabe, K., Kranjc, A., Baasansuren, J., Fukuda, M., Ngarize, S. (Eds.), 2019 Refinement to the 2006 IPCC Guidelines for National Greenhouse Gas Inventories, Volum 4. IPCC, Switzerland. Kanagawa, Japan Chapter 07 .

Jahne, B., Munnich, K.O., Bosinger, R., Dutzi, A., Huber, W., Libner, P., 1987. On parameters influencing air-water exchange. J. Geophys. Res. 92, 1937–1949. https: //doi.org/10.1029/JC092iC02p01937 .

Kelly, C.A. , Chynoweth, P. ,1981. The contributions of temperature and of the in- put of organic matter in controlling rates of sediment methanogenesis. Limnol. Oceanogr. 26 (5), 891–897 .

Keller, M., Stallard, R.F., 1994. Methane emission by bubbling from Gatun Lake. Panama. J. Geophys. Res. 99 (D4), 8307–8319. https://doi.org/10.1029/92JD02170 .

Kongkeo, H., 1997. Comparison of intensive shrimp farming systems in Indonesia, Philippines. Taiwan Thailand. Aquac. Res. 28, 789–796. http://dx.doi.org/10. 1046/j.1365-2109.1997.00943.x .

Laurion, I., Vincent, W.F., MacIntyre, S., Retamal, L., Dupont, C., Francus, P., Pienitz, R, 2010. Variability in greenhouse gas emissions from permafrost thaw ponds. Limnol. Oceanogr. 55, 115–133. https://doi.org/10.4319/lo.2010.55.1.0115 .

Li, S.Y., Bush, R.T., Santos, I.R., Zhang, Q.F., Song, K.S., Mao, R., Wen, Z.D., Lu, X.X., 2018. Large greenhouse gases emissions from China's lakes and reservoirs. Water Res. 147, 13–24. https://doi.org/10.1016/j.watres.2018.09.053 .

Liu, S.W., Hu, Z.Q., Wu, S., Li, S.Q., Li, Z.F., Zou, J.W., 2015. Methane and nitrous oxide emissions reduced following conversion of rice paddies to inland crab- fish aquaculture in southeast China. Environ. Sci. Technol. 50 (2), 633–642. https://doi.org/10.1021/acs.est.5b04343 .

Lofton, D.D., Whalen, S.C., Hershey, A.E., 2015. Vertical sediment distribution of methanogenic pathways in two shallow Arctic Alaskan lakes. Polar Biol. 38 (6), 815–827. https://doi.org/10.10 07/s0 030 0- 014- 1641- 4 .

Lorke, A., Bodmer, P., Noss, C., Alshboul, Z., Koschorreck, M., Somlai-Haase, C., Bastviken, D., Flury, S., McGinnis, D.F., Maeck, A., Müller, D., Premke, K., 2015. Technical note: Drifting versus anchored flux chambers for measuring green- house gas emissions from running waters. Biogeosciences 12 (23), 7013–7024. http://dx.doi.org/10.5194/bg- 12- 7013-2015 .

Ma, Y.C., Sun, L.Y., Liu, C.Y., Yang, X.Y., Zhou, W., Yang, B., Schwenke, G., Liu, D.L., 2018. A comparison of methane and nitrous oxide emissions from inland mixed- fish and crab aquaculture ponds. Sci. Total Environ. 637-638, 517–523. https://doi.org/10.1016/j.scitotenv.2018.05.040 .

MacIntyre, S. , Wanninkhof, R. , Chanton, J.P. , 1995. Trace gas exchange across the air-water interface in freshwater and coastal marine environment. In: Mat- son, P.A., Harriss, R.C. (Eds.), Biogenic Trace Gases: Measuring Emission from Soil and Water. Blackwell Scientific Publications Ltd, Cambridge, pp. 52–97 .

Maeck, A. , Hofmann, H. , Lorke, A. , 2014. Pumping methane out of aquatic sediments ebullition forcing mechanisms in an impounded river. Biogeosciences 11 (15), 2925–2938 .

Maher, D.T., Drexl, M., Tait, D.R., Johnston, S.G., Jeffrey, L.C., 2019. iAMES: an inex- pensive, automated methane ebullition sensor. Environ. Sci. Technol 53, 6420–6426. https://doi.org/10.1021/acs.est.9b01881 .

Matoušˇu, A. , Osudar, R. , Šimek, K. , Bussmann, I. , 2017. Methane distribution and methane oxidation in the water column of the Elbe estuary, Germany. Aquat. Sci. 79 (3), 443–458 https://doi.org/10.10 07/s0 0 027 −016 −0509 −9 .

Mattson, M.D. , Likens, G.E. , 1990. Air pressure and methane fluxes. Nature 347 (6295), 718–719 . Molnar, N., Welsh, D.T., Marchand, C., Deborde, J., Meziane, T., 2013. Impacts of shrimp farm effluent on water quality, benthic metabolism and N-dynamics in a mangrove forest (New Caledonia). Estuar. Coast. Shelf S. 117, 12–21. https://doi.org/10.1016/j.ecss.2012.07.012 .

Musenze, R.S., Grinham, A., Werner, U., Gale, D., Sturm, K., Udy, J., Yuan, Z.G., 2014. Assessing the spatial and temporal variability of diffusive methane and nitrous oxide emissions from subtropical freshwater reservoirs. Environ. Sci. Technol. 4 8, 144 99–14507. https://doi.org/10.1021/es505324h .

Natchimuthu, S., Panneer Selvam, B., Bastviken, D., 2014. Influence of weather variables on methane and carbon dioxide flux from a shallow pond. Biogeochemistry 119, 403–413. https://doi.org/10.1007/s10533- 014- 9976- z .

Natchimuthu, S., Sundgren, I., Gålfalk, M., Klemedtsson, L., Crill, P., Danielsson, ˚A., Bastviken, D., 2016. Spatio-temporal variability of lake CH 4 fluxes and its in- fluence on annual whole lake emission estimates. Limnol. Oceanogr. 61 (S1), S13–S26. https://doi.org/10.1002/lno.10222 .

Natchimuthu, S., Sundgren, I., Gålfalk, M., Klemedtsson, L., Bastviken, D., 2017. Spatiotemporal variability of lake pCO_2 and CO_2 fluxes in a hemiboreal catchment. J. Geophys. Res. Biogeosci. 122, 30–49. http://dx.doi.org/10.10 02/2016JG0 03449 .

National Oceanic and Atmospheric (NOAA), 2020. Carbon cycle greenhouse gases: Trends in CH4. Available in: https://www.esrl.noaa.gov/gmd/ccgg/trends _ ch4/

Neubauer, S.C., Megonigal, J.P., 2015. Moving beyond global warming potentials to quantify the climatic role of ecosystems. Ecosystems 18, 10 0 0–1013. https://doi.org/10.1007/s10021-015-9879-4 .

Ortega, S.H., González-Quijano, C.R., Casper, P., Singer, G.A., Gessner, M.O., 2019. Methane emissions from contrasting urban freshwaters: rates, drivers and a whole-city footprint. Glob. Change Biol. 25 (12), 4234–4243. https://doi.org/10. 1111/gcb.14799 .

Panneer Selvam, B., Natchimuthu, S., Arunachalam, L., Bastviken, D., 2014. Methane and carbon dioxide emissions from inland waters in India-implications for large scale greenhouse gas balances. Glob. Change Biol. 20 (11), 3397–3407. https: //doi.org/10.1111/gcb.12575 .

Peacock, M., Audet, J., Jordan, S., Smeds, J., Wallin, M.B., 2019. Greenhouse gas emissions from urban ponds are driven by nutrient status and hydrology. Ecosphere 10 (3), e02643. https://doi.org/10.1002/ecs2.2643 .

Pelletier, L., Strachan, I.B., Garneau, M., Roulet, N.T., 2014. Carbon release from boreal peatland open water pools: implication for the contemporary C exchange. J. Geophys. Res.-Biogeo. 119 (3), 207–222. https://doi.org/10.10 02/2013jg0 02423 .

Podgrajsek, E., Sahlee, E., Bastviken, D., Holst, J., Lindroth, A., Tranvik, L., Rutgers- son, A., 2014. Comparison of floating chamber and eddy covariance measurements of lake greenhouse gas fluxes. Biogeosciences 11 (15), 4225–4233. https: //doi.org/10.5194/bg- 11- 4225- 2014 .

Poffenbar ger, H.J., Needelman, B.A., Megonigal, J.P., 2011. Salinity influence on methane emissions from tidal marshes. Wetlands 31, 831–842. https://doi.org/ 10.1007/s13157- 011- 0197- 0 .

Ren, C.Y., Wang, Z.M., Zhang, Y.Z., Zhang, B., Chen, L., Xia, Y.B., Xiao, X.M., Doughty, R.B., Liu, M.Y., Jia, M., Mao, D.H., Song, K.S., 2019. Rapid expansion of coastal aquaculture ponds in China from Landsat observations during 1984–2016. Int. J. Appl. Earth Obs. 82, 101902. https://doi.org/10.1016/j.jag.2019. 101902 .

Rubbo, M., Cole, J., Kiesecker, J., 2006. Terrestrial subsidies of organic carbon support net ecosystem production in temporary forest ponds: evidence from an ecosystem experiment. Ecosystems 9, 1170–1176. https://doi.org/10.1007/ s10 021-0 05-0 0 09-6 .

Rosentreter, J.A., Maher, D.T., Ho, D.T., Call, M., Barr, J.G., Eyre, B.D., 2017. Spatial and temporal variability of CO 2 and CH 4 gas transfer velocities and quantification of the CH4 microbubble flux in mangrove dominated estuaries. Limnol. Oceanogr. 62 (2), 561–578. https://doi.org/10.1002/lno.104 4 4 .

Sawakuchi, H.O., Bastviken, D., Sawakuchi, A.O., Krusche, A.V., Ballester, M.V.R., Richey, J.E., 2014. Methane emissions from Amazonian rivers and their contri- bution to the global methane budget. Global Chang. Biol. 20 (9), 2829–2840. https://doi.org/10.1111/gcb.12646 .

Schrier-Uijl, A.P., Veraart, A.J., Leffelaar, P.A., Berendse, F., Veenendaal, E.M., 2011. Re- lease of CO 2 and CH 4 from lakes and drainage ditches in temperate wetlands. Biogeochemistry 102, 265–279. https://doi.org/10.1007/s10533- 010- 9440- 7 .

Sibgh, S., Bhatti, T.S., Kothari, D.P., 2007. Wind power estimation using artificial neural network. J. Energ. Eng. 133 (1), 46–52. https://doi.org/10.1061/(ASCE) 0733-9402 .

Soares, D.C.E., Henry-Silva, G.G., 2019. Emission and absorption of greenhouse gases generated from marine shrimp production (Litopeneaus vannamei) in high salinity. J. Clean. Prod. 218, 367–376. https://doi.org/10.1016/j.jclepro.2019.02.002 .

Sturm, K., Yuan, Z., Gibbes, B., Werner, U., Grinham, A., 2014. Methane and nitrous oxide sources and emissions in a subtropical freshwater reservoir, South East Queensland, Australia. Biogeosciences 11 (18), 5245–5258. https://doi.org/ 10.5194/bg- 11- 5245- 2014 .

Sun, Z.G., Wang, L.L., Tian, H.Q., Jiang, H.H., Mou, X.J., Sun, W.L., 2013. Fluxes of nitrous oxide and methane in different coastal Suaeda salsa marshes of the Yellow River estuary, China. Chemosphere 90 (2), 856–865. https://doi.org/10.1016/ j.chemosphere.2012.10.004 .

Sundh, I., Bastviken, D., Tranvik, L., 2005. Abundance, activity, and community structure of pelagic methane-oxidizing bacteria in temperate lakes. Appl. Environ. Microbiol. 71, 6746–6752. http://dx.doi.org/10.1128/AEM.71.11.6746-6752.2005 .

Tang, K.W., McGinnis, D.F., Ionescu, D., Grossart, H.-P., 2016. Methane production in oxic lake waters potentially increases aquatic methane flux to air. Environ. Sci. Technol. Lett. 3 (6), 227–233. http://dx.doi.org/10.1021/acs.estlett.6b00150 .

Tangen, B.A., Finocchiaro, R.G., Gleason, R.A., Dahl, C.F., 2016. Greenhouse gas fluxes of a shallow lake in south-central NorthDakota, USA. Wetlands 36(4), 779–787. https://doi.org/10.1007/s13157- 016- 0782- 3

Tong, C., Wang, W.Q., Zeng, C.S., Marrs, R., 2010. Methane emissions from a tidal marsh in the Min River estuary, southeast China. J. Environ. Sci. Heal. A 45, 506–516. https://doi.org/10.1080/10934520903542261 .

Tu, X.H., Xiao, B.D., Xiong, J., Chen, X., 2010. A simple miniaturised photometrical method for rapid determination of nitrate and nitrite in freshwater. Talanta 82, 976–983. https://doi.org/10.1016/j.talanta.2010.06.002 .

Verdegem, M.C.J., Bosma, R.H., 2009. Water withdrawal for brackish and inland aquaculture, and options to produce more fish in ponds with present water use. Water Policy 11 (Suppl. 1), 52–68. https://doi.org/10.2166/wp.20 09.0 03 .

Vizza, C., West, W.E., Jones, S.E., Hart, J.A ., Lamberti, G.A ., 2017. Regulators of coastal wetland methane production and responses to simulated global change. Biogeo- sciences 14, 431–446. https://doi.org/10.5194/bg- 14- 431- 2017 .

Walter, K.M., Chanton, J.P., Chapin, F.S., Schuur, E.A.G., Zimov, S.A., 2008. Methane production and bubble emissions from Arctic lakes: isotopic implications for source pathways and ages. J. Geophys. Res. 113, G00a08. http://dx.doi.org/10. 1029/20 07jg0 0 0569 .

Wang, H.J., Lu, J.W., Wang, W.D., Yang, L.Y., Yin, C.Q., 2006. Methane fluxes from the littoral zone of hypereutrophic Taihu Lake, China. J. Geophys. Res. 111, D17109. http://dx.doi.org/10.1029/20 05JD0 06864 .

Wang, Q. , Liu, H. , Sui, J. , 2018. Mariculture: Developments, present status and prospects. In: Gui, J.F., Tang, Q., Li, Z., Liu, J., De Silva, S.S. (Eds.), Aquaculture in China: Success Stories and Modern Trends. John Wiley & Sons Ltd, Hoboken, N.J., pp. 38–54 .

Wang, X.F., He, Y.X., Yuan, X.Z., Chen, H., Peng, C.H., Yue, J.S., Zhang, Q.Y., Diao, Y.B., Liu, S.S., 2017. Greenhouse gases concentration s and fluxes from subtropical small reservoirs in relation with watershed urbanization. Atmos. Environ. 154, 225–235. http://dx.doi.org/10.1016/j.atmosenv.2017.01.047 .

Wanninkhof, R., 1992. Relationship between wind speed and gas exchange over the ocean. J. Geophys. Res. Oceans 97 (C5), 7373–7382. https://doi.org/10.1029/ 92JC00188 .

Wassmann, R. , Neue, H.U. , Bueno, C. , Lantin, R.S. , Alberto, M.C.R. , Buendia, L.V. , Bron- son, K. , Papen, H. , Rennenberg, H. , 1998. Methane production capacities of different rice soils derived from inherent and exogenous substrates. Plant Soil 203, 227–237 .

Wei, D., Wang, X.D., 2017. Uncertainty and dynamics of natural wetland CH_4 release in China: research status and priorities. Atmos. Environ. 154, 95–105. https://doi.org/10.1016/j.atmosenv.2017.01.038 .

Welti, N., Hayes, M., Lockington, D., 2017. Seasonal nitrous oxide and methane emissions across a subtropical estuarine salinity gradient. Biogeochemistry 132, 55–69. https://doi.org/10.1007/s10533- 016- 0287- 4 .

Wik, M., Crill, P.M., Varner, R.K., Bastviken, D., 2013. Multiyear measurements of ebullitive methane flux from three subarctic lakes. J. Geophys. Res.-Biogeo. 118, 1307–1321. http://dx.doi.org/10.1002/jgrg.20103 .

Wilson, B.J., Mortazavi, B., Kiene, R.P., 2015. Spatial and temporal variability in carbon dioxide and methane exchange at three coastal marshes along a salinity gradient in a northern Gulf of Mexico estuary. Biogeochemistry 123, 329–347. https://doi.org/10.1007/s10533-015-0085-4 .

Wu, S., Hu, Z.Q., Hu, T., Chen, J., Yu, K., Zou, J.W., Liu, S.W., 2018. Annual methane and nitrous oxide emissions from rice paddies and inland fish aquaculture wet- lands in southeast China. Atmos. Environ. 175, 135–144. https://doi.org/10.1016/ j.atmosenv.2017.12.008 .

Wu, S., Li, S.Q., Zou, Z.H., Hu, T., Hu, Z.Q., Liu, S.W., Zou, J.W., 2019. High methane emissions largely attributed to ebullitive fluxes from a subtropical river draining a rice paddy watershed in China. Environ. Sci. Technol. 53, 349–3507. https: //doi.org/10.1021/acs.est.8b05286 .

Xiao, Q.T., Zhang, M., Hu, Z.H., Gao, Y.Q., Hu, C., Liu, C., Liu, S.D., Zhang, Z., Zhao, J.Y., Xiao, W., Lee, X., 2017. Spatial variations of methane emission in a large shallow eutrophic lake in subtropical climate. J. Geophys. Res. Biogeosci. 122 (7), 1597–1614. https://doi.org/10.10 02/2017JG0 03805 .

Xie, B., Yu, K.J., 2007. Shrimp farming in China: Operating characteristics, environmental impact and perspectives. Ocean Coast. Manage. 50 (7), 538–550. https://doi.org/10.1016/j.ocecoaman.20 07.02.0 06 .

Xing, Y.P., Xie, P., Yang, H., Ni, L.Y., Wang, Y.S., Tang, W.H., 2004. Diel variation of methane fluxes in summer in a eutrophic subtropical lake in China. J. Freshwat. Ecol. 19, 639–644. https://doi.org/10.1080/02705060.2004.9664745 .

Xing, Y.P., Xie, P., Yang, H., Ni, L.Y., Wang, Y.S., Rong, K.W., 2005. Methane and carbon dioxide fluxes from a shallow hypereutrophic subtropical lake in China. Atmos. Environ. 39, 5532–5540. https://doi.org/10.1016/j.atmosenv.2005.06.010 .

Yang, H., 2014. China must continue the momentum of green law. Nature 509 (7502). 535-353 https://doi.org/10.1038/509535a .

Yang, H., Flower, R.J., 2012. Potentially massive greenhouse-gas sources in proposed tropical dams. Front. Ecol. Environ. 10, 234–235. https://doi.org/10.1890/12.WB. 014 .

Yang, H., Xie, P., Ni, L., Flower, R.J., 2011. Underestimation of CH_4 emission from freshwater lakes in China. Environ. Sci. Technol. 45, 4203–4204. https://doi.org/ 10.1021/es2010336 .

Yang, P., Lai, D.Y.F., Jin, B.S., Bastviken, D., Tan, L.S., Tong, C., 2017a. Dynamics of dissolved nutrients in the aquaculture shrimp ponds of the Min River estuary, China: Concentrations, fluxes and environmental loads. Sci. Total Environ. 603- 604, 256–267. http://dx.doi.org/10.1016/j.scitotenv.2017.06.074 .

Yang, H., Andersen, T., Dörsch, P., Tominaga, K., Thrane, J.-E., Hessen, D.O., 2015. Greenhouse gas metabolism in Nordic boreal lakes. Biogeochemistry 126, 211–225. https://doi.org/10.1007/s10533-015-0154-8 .

Yang, P., Bastviken, D., Jin, B.S., Mou, X.J., Tong, C., 2017b. Effects of coastal marsh conversion to shrimp aquaculture ponds on CH_4 and N_2O emissions. Estuar. Coast. Shelf S. 199, 125–131. https://doi.org/10.1016/j.ecss.2017.09.023 .

Yang, P., Zhang, Y.F, Lai, D.Y.F., Tan, L.S., Jin, B.S., Tong, C., 2018. Fluxes of carbon dioxide and methane across the water–atmosphere interface of aquaculture shrimp ponds in two subtropical estuaries: The effect of temperature, substrate, salinity and nitrate. Sci. Total Environ. 635, 1025–1035. https://doi.org/10.1016/j. scitotenv.2018.04.102 .

Yang, P., Zhang, Y., Yang, H., Zhang, Y.F., Xu, J., Tan, L.S., Tong, C., Lai, D.Y.F., 2019a. Large fine-scale spatiotemporal variations of CH_4 diffusive fluxes from shrimp aquaculture ponds affected by organic matter supply and aeration in South- east China. J. Geophys. Res.-Biogeo. 124, 1290–1307. https://doi.org/10.1029/ 2019JG005025 .

Yang, P., Wang, M.H., Lai, D.Y.F., Chune, K.P., Huang, J.F., Wan, S.A., Bastviken, D., Tong, C., 2019b. Methane dynamics in an estuarine brackish *Cyperus malaccensis* marsh: Production and porewater concentration in soils, and net emissions to the atmosphere over five years. Geoderma 337, 132–142. https://doi.org/10.1016/ j.geoderma.2018.09.019 .

Yang, P., Lai, D.Y.F., Yang, H., Tong, C., Lebel, L., Huang, J., Xu, J., 2019c. Methane dynamics of aquaculture shrimp ponds in two subtropical estuaries, southeast China: Dissolved concentration, net sediment release, and water oxidation. J. Geophys. Res.-Biogeo. 124, 1430–1445. https://doi.org/10.1029/2018JG004794 .

Yang, P., Yang, H., Lai, D.Y.F., Guo, Q.Q., Zhang, Y.F., Tong, C., Xu, C.B., Li, X.F., 2020a. Large contribution of non-aquaculture period fluxes to the annual N_2O emissions from aquaculture ponds in Southeast China. J. Hydrol. 582, 124550. https://doi.org/10.1016/j.jhydrol.2020.124550 .

Yang, P., Zhang, Y., Bastviken, D., Lai, D.Y.F., Yang, H., Zhang, Y.F., Guo, Q.Q., Tan, L.S., Tong, C., 2020b. Large increase in diffusive greenhouse gas fluxes from subtropical shallow aquaculture ponds during the passage of typhoons. J. Hydrol. 583, 124643. https://doi.org/10.1016/j.jhydrol.2020.124643 .

Yuan, J.J., Xiang, J., Liu, D.Y., Kang, H., He, T.H., Kim, S., Lin, Y.X., Freeman, C., Ding, W.X., 2019. Rapid growth in greenhouse gas emissions from the adoption of industrial-scale aquaculture. Nat. Clim. Change 9 (4), 318–322. https: //doi.org/10.1038/s41558- 019- 0425- 9 .

Yuan, Y. , Cai, J. , Leung, P.S. , 2006. An overview of China's cultured shrimp industry. In: Leung, P.S., Engle, C. (Eds.), Shrimp Culture: Economics, Market, and Trade. Blackwell Publishing, Oxford, U.K., pp. 197–222 .

Zhang, Y.F., Yang, P., Yang, H., Tan, L.S., Guo, Q.Q., Zhao, G.H., Li, L., Gao, Y.C., Tong, C., 2019. Plot-scale spatiotemporal variations of CO_2 concentration and flux across water-air interfaces at aquaculture shrimp ponds in a subtropical estuary. Environ. Sci. Pollut. R. 26, 5623–5637. https://doi.org/10.1007/ s11356- 018- 3929- 3 .

Zhou, Y.Q., Zhou, L., Zhang, Y.L., de Souza, J.G., Podgorski, D.C., Spencer, R.G.M., Jeppesen, E., Davidson, T.A., 2019. Autochthonous dissolved organic matter potentially fuels methane ebullition from experimental lakes. Water Res. 166, 115048. https://doi.org/10.1016/j.watres.2019.115048 .

Zou, X.X., Li, Y.E, Li, K., Cremades, R., Gao, Q.Z., Wan, Y.F., Qin, X.B., 2015. Greenhouse gas emissions from agricultural irrigation in China. Mitig. Adapt. Strateg. Glob. Change 20 (2), 295–315. https://doi.org/10.1007/s11027- 013- 9492- 9 .

Zhao, Y., Wu, B.F., Zeng, Y., 2013. Spatial and temporal patterns of greenhouse gas emissions from Three Gorges Reservoir of China. Biogeosciences 10, 1219–1230. https://doi.org/10.5194/bg-10-1219-2013 .

Zheng, H., Zhao, X.J., Zhao, T.Q., Chen, F.L., Xu, W.H., Duan, X.N., Wang, X.K., Ouyang, Z.Y., 2011. Spatial-temporal variations of methane emissions from the Ertan hydroelectric reservoir in southwest China. Hydrol. Process. 25, 1391–1396. https://doi.org/10.1002/hyp.7903 .

Zhu, D., Wu, Y., Chen, H., He, Y.X., Wu, N., 2016. Intense methane ebullition from open water area of a shallow peatland lake on the eastern Tibetan Plateau. Sci. Total Environ. 542, 57–64. https://doi.org/10.1016/j.scitotenv.2015.10.087.